Fault Specific GIS Based Seismic Hazard Maps for the Attica Region, Greece

Deligiannakis, G. [(a)], Papanikolaou, I.D. [(a,b)], Roberts, G. [(b)]

[(a)] Mineralogy-Geology Laboratory, Department of Natural Resources Development and Agricultural Engineering, Agricultural University of Athens, 75 Iera Odos, 118-55, Athens, Greece. Email: gdeligian@aua.gr

[(b)] Department of Earth Sciences Birkbeck College and University College London, WC 1E 6BT, London UK. Emails: i.papanikolaou@ucl.ac.uk, gerald.roberts@ucl.ac.uk

Abstract

Traditional seismic hazard assessment methods are based on the historical seismic records for the calculation of an annual probability of exceedance for a particular ground motion level. A new fault specific seismic hazard assessment method is presented, in order to address problems related to the incompleteness and the inhomogeneity of the historical records and to obtain higher spatial resolution of hazard. This method is applied to the region of Attica, which is the most densely populated area in Greece, as nearly half of the country's population lives in Athens and its surrounding suburbs, in Greater Athens Area. The methodology is based on a database of 22 active faults that could cause damage to Attica in case of seismic rupture. This database provides information about the faults slip rates, lengths and expected magnitudes. The final output of this method are four fault specific seismic hazard maps, showing the recurrence of expected intensities that each locality in the map has been shaken at. These maps offer a high spatial resolution, as they consider the surface geology. Despite the fact that almost half of the Attica region lies on the lowest seismic risk zone according to the official seismic hazard zonation of Greece, different localities have repeatedly experienced strong ground motions during the last 15 kyrs. Moreover, the maximum recurrence for each intensity occurs in different localities across Attica. Highest recurrence for intensity VII (151-156 times over 15

kyrs, or up to 96 year return period) is observed in the central part of the Athens basin. The maximum intensity VIII recurrence (114 times over 15 kyrs, or up to 131 year return period) is observed in the western part of Attica, while the maximum intensity IX (73-77/15kyrs, or 195 year return period) and X (25-29/15kyrs, or 517 year return period) recurrences are observed near the South Alkyonides fault system, which dominates the strong ground motions hazard in the western part of the Attica mainland.

Keywords

Athens, active faults, slip rates, earthquakes, intensity, faults database

1. Introduction

~~Greece is prone to various natural disasters, such as wildfires, floods, landslides and earthquakes, due to the special environmental and geological conditions dominating in tectonic plate boundaries. Seismic is the predominant risk, in terms of damages and casualties in the Greek territory (PreventionWeb, 2011).~~

During the last 500 years, more than 170 destructive earthquakes occurred in Greece and the surrounding area, with mean annual casualties of 17 fatalities and 92 wounded (Papazachos and Papazachou, 2003). The historical record of earthquakes in Greece is compiled by various researchers (Galanopoulos, 1961, Makropoulos and Burton, 1984, Papazachos and Papazachou, 1997), providing useful data in seismic hazard assessment of Greece.

Greece has one of the longest historical catalogues worldwide with the oldest recorded events in 550 B.C. However, there is an incompleteness and inhomogeneity

of geographical and temporal coverage in terms of the seismic record, so that this catalogue is considered complete for events M≥7.3 since 1500 and for M≥6.5 only since 1845 (Papazachos, et al. 2000). However, the recurrence interval of particular faults ranges from a few hundred years to several thousands of years (Goes 1996, Yeats and Prentice 1996, Machette 2000). Regarding the Attica region, recurrence intervals vary from a few hundred years for the highly active South Alkyonides Fault (Collier, et al. 1998), up to thousands of years, as shown in the Kaparelli fault, which was reactivated in 1981, after being inactive for several thousands of years ~~approximately 10 kyrs~~ (Benedetti, et al. 2003; Chatzipetros, et al. 2005; Kokkalas, et al. 2007). Thus, historical earthquake catalogues are generally too short compared to the recurrence intervals of faults. The latter implies that the sample from the historical record is incomplete and that a large number of faults would not have ruptured during the completeness period of the historical record (e.g. Grützner, et al. 2013). Further uncertainties are related to the epicenters location, even for instrumentally recorded earthquakes (Papanikolaou, et al. 2015). The errors can reach up to 20 km for the older events (1965-1980) and up to 10km for the most recent ones (Papazachos, et al. 2000). Larger uncertainties result for the older events approximate epicentral locations. For the period 1901-1964 the errors can be up to 30km but they can reach up to 50km for the older events (before 1900) when the number of available macroseismic information is less than 5 (Papazachos, et al. 2000, Stucchi, et al. 2012). Indeed, recorded events in the Attica region are an example, as the uncertainty on the epicentral locations for the most recent Athens 1999 Mw 5.9 earthquake, which are derived from different papers and catalogues, exceed 5km. For the older Oropos 1938 Mw 6.0 event, the epicenters in two different catalogues are located 12km away of each other.

New Seismic Hazard Assessment methodologies tend to follow fault specific approaches where seismic sources are geologically constrained active faults (WGCEP, 1990, 1999, 2002, 2008; Ganas and Papoulia, 2000; Boncio, et al. 2004; Roberts, et al. 2004; Papanikolaou and Papanikolaou, 2007; Pace, et al. 2010; Stein, et al. 2012; Papanikolaou, et al. 2013). These fault specific approaches are used in order to address problems related to the historical records incompleteness, obtain higher spatial resolution and calculate realistic source locality distances, since seismic sources are very accurately located. Fault specific approaches provide quantitative assessments as they measure fault slip rates from geological data, providing a more reliable estimate of seismic hazard than the historical earthquake record (e.g. Yeats and Prentice, 1996; Papoulia, et al. 2001; Michetti, et al. 2005). Geological data have the potential to extend the history of slip on an active fault back many thousands of years, a time span that generally encompasses a large number of earthquake cycles (Yeats and Prentice 1996), and thus elucidates the long-term pattern of fault-slip. In addition, geologic fault slip-rate data offer complete spatial coverage, providing higher spatial resolution than traditional seismic hazard maps based on historical/instrumental records (Boncio, et al. 2004, Roberts, et al. 2004, Pace, et al. 2010, Papanikolaou, et al. 2013). For land-use planning and critical facilities or insurance risk evaluation purposes, a higher spatial resolution is also desirable (Grützner, et al. 2013).

As a result, there is an emerging tendency for incorporating fault specific information relating both to the identification and mapping of active faults, as well as extracting information regarding the recurrence interval of associated potential earthquakes (Papanikolaou, et al 2015).

~~1.1 Existing seismic hazard models~~

~~The probabilistic seismic hazard analyses calculate the probability of exceeding different levels of ground motion (intensity or acceleration) by considering the earthquake location, timing and size. These analyses are based on the likelihood of occurrence of various magnitude earthquakes and their contributions to ground motion hazards. On the other hand, deterministic analyses only consider ground motions or highest intensities due to the maximum credible earthquake (Youngs and Coppersmith, 1985).~~

~~The results of probabilistic seismic hazard analysis are usually consisted of maps at a given level of probability, based on a combination of the earthquake frequency-magnitude distribution, ground motion attenuation data, and local site conditions (Main, 1996). The general procedure followed in probabilistic seismic hazard analysis includes the individual steps of seismic zoning, estimating the recurrence, and fitting a local attenuation law to the ground motion in order to calculate an annual probability of exceedance of a particular level of ground motion (Reiter, 1990). The primary probabilistic tool for projecting future events is the seismicity record (Yeats, et al. 1997).~~

2. Methodology

A fault specific seismic hazard assessment approach was used for the seismic hazard assessment of the Attica region. The method of seismic hazard mapping from geological fault throw-rate data was firstly introduced by Papanikolaou (2003) and Roberts, et al. (2004). It consists of the combination of the following four major factors:

1. compilation of a fault database, that includes the identification of seismic sources, determination of fault lengths and their characteristics regarding their kinematics and slip rates which govern earthquake recurrence.
2. empirical data which combine fault rupture lengths, earthquake magnitudes and coseismic slip relationships (Wells and Coppersmith, 1994; Pavlides and Caputo, 2004).
3. the radii of VI, VII, VIII, and also IX isoseismals on the Modified Mercalli (MM) intensity scale, within which horizontal ground accelerations exceed 500cm/sec^2 in the Greek territory (Theodulidis and Papazachos, 1992) causing damage even to well-constructed buildings (Rieter, 1990).
4. Attenuation - amplification functions for seismic shaking on bedrock compared to basin filling sediments (Degg 1992).

In detail, fault specific Seismic Hazard Mapping methodology can be displayed in the following steps (see also Papanikolaou 2003, Roberts, et al. 2004, Papanikolaou, et al. 2013):

2.1 Active faults identification

When seismic hazard is estimated for a wide region, all the seismic sources must be identified. All active faults that affect the study area must be accurately mapped, as they are going to be analyzed in the next steps. Geological and geomorphological studies are often the primary basis for locating potential seismic sources (Wesnousky, 1987). A large set of data are used for understanding the current tectonic regime and rates of activity, including: aerial photographs, remote sensing data (such as those derived from satellite imagery), GPS and interferometry data, strain rate measurements, mapping and analysis of Quaternary formations and/or land - forms

(such as terrace analysis and investigation of drainage network evolution), and pedological and sedimentological studies. Usually, it is necessary to perform detailed geomorphological-geological mapping, geophysical prospecting, or subsurface investigation to fully characterize the identified structures (Michetti, et al. 2005). The usual criteria for identifying active faults are the Quaternary deposits disruption, rivers or tributaries delimitation and creation of characteristic and recognizable set of geomorphologic landscapes.

The detailed data for faults characteristics were derived from scientific articles, onshore and offshore neotectonic maps and fieldwork observations. In general, two type of sources were used for the active faults determination:

a) Already published literature regarding location and fault activity.

   The published papers of researchers working on the active tectonics of Attica and the surrounding areas were used for the majority of the active faults (19 out of 22) regarding the compilation of the database. For 13 out of the 22 faults (Fault id numbers 1-5, 8-11, 13-15 and 19 of the database, see Figure 3 and Table 3) information regarding fault geometry and slip rates were extracted from the existing literature (see Table 3 for details on corresponding literature) ~~(Pantosti, et al. 1996; Collier, et al. 1998; Morewood & Roberts, 2001; Pavlides, et al. 2002; Goldsworthy, et al. 2002; Benedetti, et al. 2003; Ganas, et al. 2004; Ganas, et al. 2005; Kokkalas, et al. 2007; Papanikolaou & Papanikolaou, 2007; Sakellariou, et al. 2007; Rontoyianni & Marinos, 2008; Tsodoulos, et al. 2008; Roberts, et al. 2009; Roberts, et al. 2011 and Grutzner, et al. 2016)~~. Moreover, onshore and offshore neotectonic maps provided information about the fault geometry and slip rate. The offshore neotectonic maps of the Saronikos and the Southern Evoikos Gulfs (Papanikolaou, et al. 1989a; Papanikolaou, et al. 1989b)

were utilized for the depiction of the 6 offshore active faults (Fault id numbers 12, 16-18, 21-22) and their characteristics.

b) Fieldwork with in situ geomorphological interpretations.

Field research was conducted for faults 6-7 and 20, in order to estimate fault lengths, finite throw and slip rate values.

2.2 Fault lengths determination

~~The lengths of active faults are usually determined from: a) geological cross-sections made from published geological maps; b) fault slip directions, as they vary with throw, converging towards the center of the hanging wall (Roberts, 1996; Roberts and Ganas, 2000); c) abrupt slope changes; d) deformation rates extracted either from trench-sites or from geomorphic observations of offset features of known age e) profile analysis of catchments crossing the fault~~. Since fault length was used to determine the expected earthquake magnitude (Figure 4), each one of the active faults that could affect Attica region in case of earthquake rupture was mapped in GIS environment (see Chapter 4 for constraints based on errors and assumptions).

Despite the fact that 1:50.000 scale geological maps cover nearly the whole Greek territory, faults depiction is usually restricted to small or inactive structures with no contribution to seismic hazard. Fault lengths for the faults 6-7 and 20 were determined using a combination of geomorphological and geological criteria. In addition to the in situ interpretations, hillshade and slope maps were utilized so that the overall topographic imprint would be observed. In addition to that, geological cross-sections in the tips of these faults were used to identity the sediments offset, which allowed a detailed mapping of the fault lengths.

2.3 Registration of fault throw-rate data

Throw-rates are measured values derived from geological data, such as postglacial scarps analysis, palaeoseismological research and geomorphological interpretations. Fault throw-rate values are essential for the Seismic Hazard Assessment, as high values indicate shorter recurrence intervals between earthquake events, implying increased fault activity (Cowie and Roberts 2001, Roberts, et al. 2004). The determination of fault throw rates was based on the published literature findings were applicable. For faults id 1-3, 5, 8-9 and 14-15 throw rates were extracted from the well – described and constrained values already presented in the literature (Benedetti, et al, 2003; Ganas, et al. 2005; Chatzipetros, et al. 2005; Papanikolaou & Papanikolaou, 2007; Sakellariou, et al. 2007; Grutzner, et al, 2016). Faults derived from the neotectonic maps did not have an assigned throw rate value. For these faults we used the average thickness of the sediments versus their age, for the extraction of their long term slip rate. Slip rate values extracted from fieldwork were attributed to the maximum scarp heights, assuming that they represent the maximum finite throw since over a fixed time period (i.e. the last glaciation).

2.4 Conversion of throw-rates into earthquake frequencies

~~Now that fault lengths, throws and throw-rates are known, throw-length profiles can be constructed for given time periods (e.g. since the last glaciation).~~ Assuming a triangular throw profile for the faults (Cowie and Shipton, 1998) and earthquake surface ruptures, and that the maximum throw is observed at the center of the fault, the number of surface faulting earthquakes of fixed size can be calculated for each one of the faults in a certain time period. Throws in these profiles represent the slip that each fault has accumulated during the last 15 kyrs and most of them have been

220 extracted from geomorphic observations of offset postglacial features. However, for
221 the South Alkyonides Fault, the surface ruptures used (25km) are shorter than the total
222 length of the fault, as the 1981 earthquakes did not rupture the entire length of the
223 South Alkyonides Fault (Roberts, 1996). This results to the assumption that the South
224 Alkyonides fault produces earthquakes of smaller magnitude (e.g. Ms = 6.7) more
225 frequently, rather than larger earthquakes that rupture the total fault length but in
226 longer recurrence time. Thus, it is assumed that this fault ruptures in floating
227 earthquakes, which are distributed around a mean magnitude of fixed size (e.g.
228 Papanikolaou, et al. 2013). As a result, by comparing the areas of triangles for faults
229 and ruptures, the number of earthquakes each fault has experienced during the last 15
230 kyrs can be calculated (example shown in Figure 1a,b). ~~The distribution of the~~
231 ~~associated hypothetical epicenters along strike the fault is made using the~~
232 ~~mathematical formula of Papanikolaou (2003).~~

233 **2.5 Earthquake distribution along strike the fault**

234 After calculating how many earthquakes of certain size each fault has experienced
235 during the last 15 kyrs, modeled earthquakes have to be distributed according to the
236 fault throw variation along strike each fault trace. The aim is to extract the earthquake
237 density along strike the fault. The distribution of the associated hypothetical
238 epicenters along strike the fault is made using the mathematical formula of
239 Papanikolaou (2003), as illustrated in Figure 1c.

240 **2.6 Production of isoseismals**

241 Earthquakes are not uniformly distributed throughout the continental crust, but are
242 overwhelmingly concentrated in the upper 10-15 km, close to the base of the
243 seismogenic layer, with the lower continental crust remaining aseismic (Chen and

Molnar, 1983; Sibson, 1984). Moreover, large seismogenic faults on the continents appear to be restricted to a dip range between 30° - 60° (Jackson and White, 1989, Chen and Molnar, 1983). The thickness of the seismogenic layer, as well as the dip angles of normal faults, constrained the placement of the hypothetical epicenters ~~The hypothetical epicenters projected across the active faults~~. Assuming 50° - 55° dipping faults and hypocenters at the depth of 10 km, they were plotted 7 - 8.5 km away from the fault in the hanging wall. ~~Map plotting of the epicenters was made using the Buffer Tool, which was set to expand the buffer zone towards the fault's hanging wall.~~

The active faults were grouped in two sets, depending on their length, which correlates to the earthquake magnitude they can produce, as shown by Wells & Coppersmith (1994) and Pavlides & Caputo (2004). For faults shorter than 16km we used an average magnitude of 6.25 ± 0.15, since faults from 9.2 km up to 16 km can produce earthquakes that lie within a range of magnitude 6.1 – 6.4 (Wells & Coppersmith, 1994). Consequently, following the same empirical regressions of surface rupture length and magnitude, faults longer than 16 km produce earthquakes of magnitudes that exceed Ms=6.5. However, it is possible that faults around 25 km – 40 km length could rupture in sub-events or break parts rather than the entire fault lengtht, thus producing earthquakes around Ms 6.5 – Ms 6.7 (e.g. Roberts, 1996; Roberts et al., 2004). For each group, we used the Theodulidis (1991) attenuation relationships between earthquake magnitude and intensities distribution for the production of the modeled isoseismals (Table 1). It is assumed that the Earth is homogeneous and isotropic so body waves would have spherical wave fronts (Figure 1d).

Table 1: Radii of the isoseismals for the active faults in Attica, based on the Theodulidis (1991) attenuation relationships. Intensity IX is not expected in firm sediments affected by faults shorter than 16km.

Faults group by earthquake magnitude	**Intensity (MM)**			
	IX	**VIII**	**VII**	**VI**
6.65 ± 0.15 (6.5 – 6.8)	11km	25km	44km	74km
6.25 ± 0.15 (6.1 – 6.4)	-	15km	31km	53km

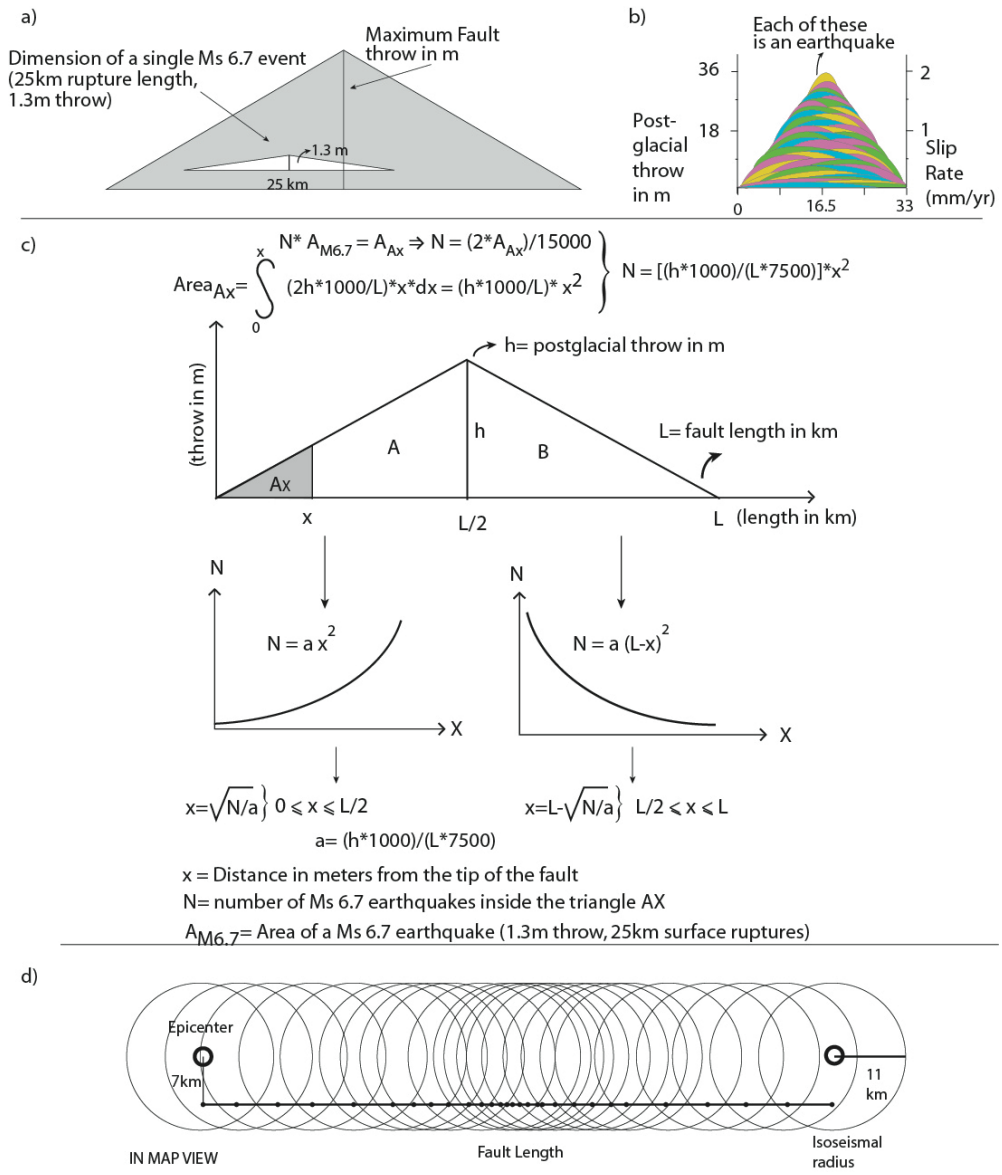

Figure 1: Schematic representation for the construction of the hazard map, modified after Papanikolaou (2003) and Roberts, et al. (2004). a) The concept of the methodology for one of the 22 faults in Attica (South Alkyonides Fault). Assuming a triangular throw profile for the faults and ruptures and that the maximum throw is observed at the centre of the fault, the number of surface faulting earthquakes of Ms=6.7 can be calculated. b) Throw in this profile represents the slip that the fault has accumulated during the post-glacial period (since 15 kyr ago±3 kyr). c) Mathematical formula describing the earthquake distribution along strike each active fault. The distance (x) of each earthquake point from the tip of the fault is calculated. Each fault is divided in two halves (triangles A and B) and the corresponding formula is applied for each one of them. d) Epicentres are plotted 7 km away from the fault in the hanging wall and circles with 11 km radius of intensity IX (representing "isoseismals") are added. Geology is not yet taken into account.

2.7 Counting and contouring the number of times each locality has been shaken.

Every intensity coverage was represented as a separate raster, so that no overlapping occurred between raster coverages of different intensities around the same modeled epicenter. Buffer zones were created around each hypothetical epicenter for every modeled intensity, using the ranges displayed in Table 1. These buffer zones were converted to raster coverages and attributed by new values. Then, all these coverages, centered to the hypothetical epicenters, were added in separate map views for each intensity scenario, representing areas that receive enough energy to shake at intensities VI – IX.

The outcome of this process is four individual maps, showing how many times each locality receives enough energy to shake at intensities VI - IX in 15kyrs, assuming homogenous bedrock geology, spherical wave fronts for body waves and isoseismal ranges as shown in Table 1. The hazard distribution varies along strike each fault, so that over long time periods the hangingwall center of a fault receives most of the seismic energy, in contrast to fault tips where the hazard is considerably lower.

2.8 Amplify/Attenuate with the bedrock geology

The modeled intensity coverages are attenuated/amplified according to the ~~bedrock geology~~ surface geologic conditions, providing the expected intensities for each geological formation. The simple attenuation model decreases the intensity by: i) a single value, if two localities are equidistant from an epicenter, but one lies on Mesozoic or Tertiary limestone and the other lies on flysch/foredeep deposits and ii) two single values if two localities are equidistant from an epicenter, but one lies on Mesozoic limestone and the other lies on Quaternary sediments (Table 2).

295 In the case of the Attica Region, the Quaternary deposits increase the intensity by a
296 single value. The flysch/foredeep deposits will cause no alterations in the intensity
297 value, while the bedrock (mostly Mesozoic or Tertiary limestone) will decrease the
298 intensity by one value (Figure 2). The input data for the surface geology is extracted
299 from: a) the 1:25,000 Earthquake Planning and Protection Organization (EPPO)
300 detailed geotechnical map for the Athens Metropolitan Area (Marinos, et al. 1999a),
301 b) the 12 1:50,000 geological maps of IGME (Tataris, et al. 1966; Gaitanakis, et al.
302 1985; Latsoudas, 1992; Katsikatsos, et al. 1986; Katsikatsos, 2000; Parginos, et al.
303 2007; Katsikatsos, 2002; Katsikatsos, 1991; Dounas, 1971; Mpornovas, et al. 1984;
304 Gaitanakis, et al. 1984; Gaitanakis, 1982) for the rest of the Attica mainland.
305

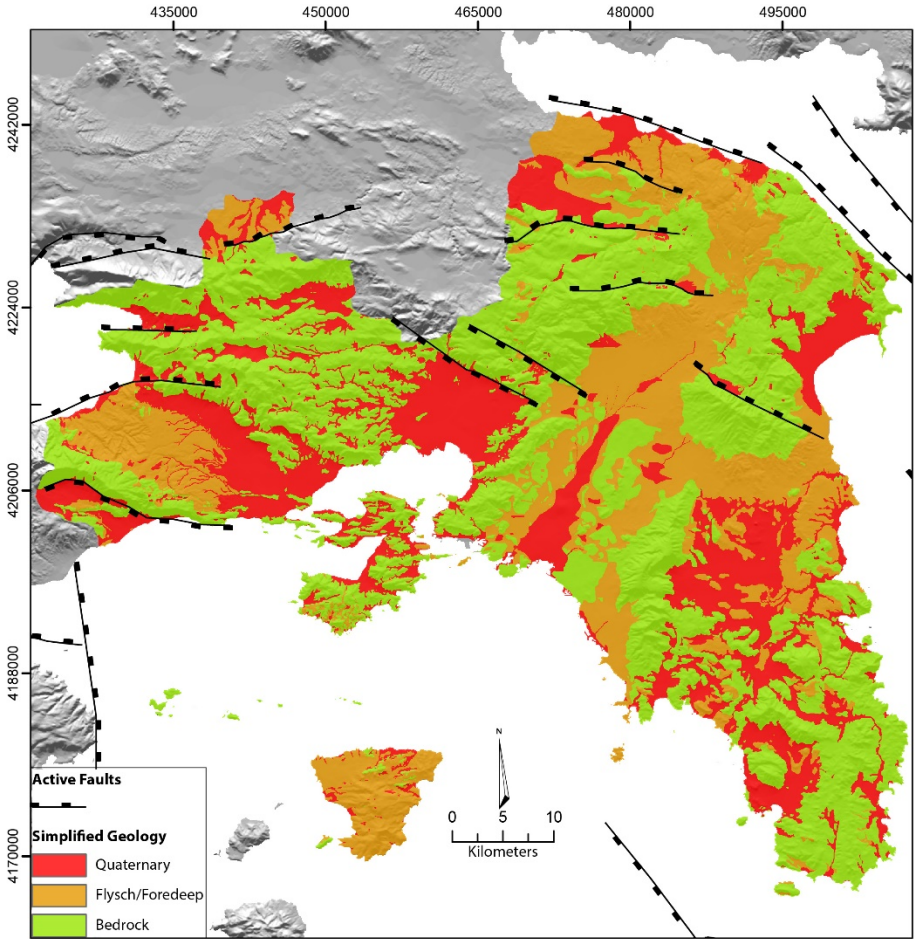

Figure 2: Simplified geological map of the area of Attica, based on 1:50,000 scale geological maps of IGME and the 1:25,000 scale Earthquake Planning and Protection Organization (EPPO) detailed geotechnical map for the Athens Metropolitan Area (Marinos, et al. 1999a).

306

307 Table 2: Average intensity changes depending on different types of surface geology, proposed by

308 Degg (1992).

Subsoil	**Average change in intensity**
Rock (e.g. limestone, granite, gneiss, basalt)	-1
Firm sediments	0
Loose sediments (e.g. sand, alluvial deposits)	+1

309 Overall, the produced hazard maps incorporate information on bedrock geology and

310 its contribution to spatial variations in ground shaking intensity.

3. Results

3.1 Active Faults Database

The active faults database contains 22 faults that: a) are long enough to produce surface ruptures and b) can sustain damage in the Attica mainland in case of earthquake rupture (Figure 3).

Fault lengths and their characteristics regarding their kinematics and slip rates are shown in Table 3.

The average expected earthquake magnitude is Mw 6.5, based on empirical relationships between rupture lengths and earthquake magnitudes. However, these faults are located away of the Athens plain, except for the southeastern tip of the Fili fault (id = 15 in Table 3, see Figure 3). As a result, seismic hazard in the Athens Plain is less significant. Moreover, most of the densely inhabited areas in the Greater Athens Area lay on the footwall of the neighboring active faults (id = 3, 4 on Table 3, see Figures 3, 4). Fault lengths vary from 9 up to 35km. Faults that exceed 30km in length were assumed to rupture in floating earthquakes of magnitude Ms = 6.65±0.15. As a result, the expected earthquake magnitude of the South Alkyonides Fault system (id = 8 in Table 3) is not proportional to its length (Roberts, 1986). Instead, we modelled floating earthquakes of magnitude 6.7 along strike the fault, which is in agreement with the 1981 earthquake (Jackson, et al. 1982).

The majority of the active faults that affect the region of Attica do not exceed the relatively low slip-rate values of 0.3mm/yr. However, the faults activated during the 1981 earthquakes events (South Alkyonides Fault segments) reach or exceed slip-rate values of 2mm/yr, thus the mean slip-rate value of the faults that affect Attica is ~0.38mm/y (Figure 4b).

335

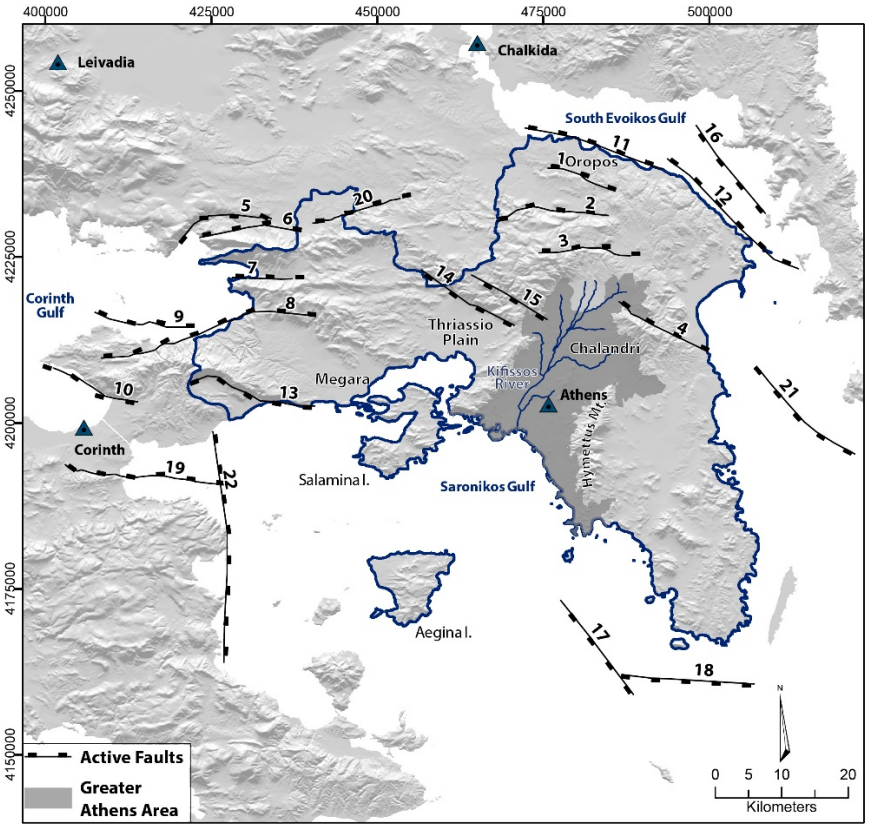

Figure 3: Map of active faults that can sustain damage within the region of Attica. No faults are located in the Athens Plain, except for the southeastern tip of the Fili fault (id = 15 on Table 3), but with low slip rate faults (see Figure 4b). Fault labels refer to the Id numbers on (Table 3).

336

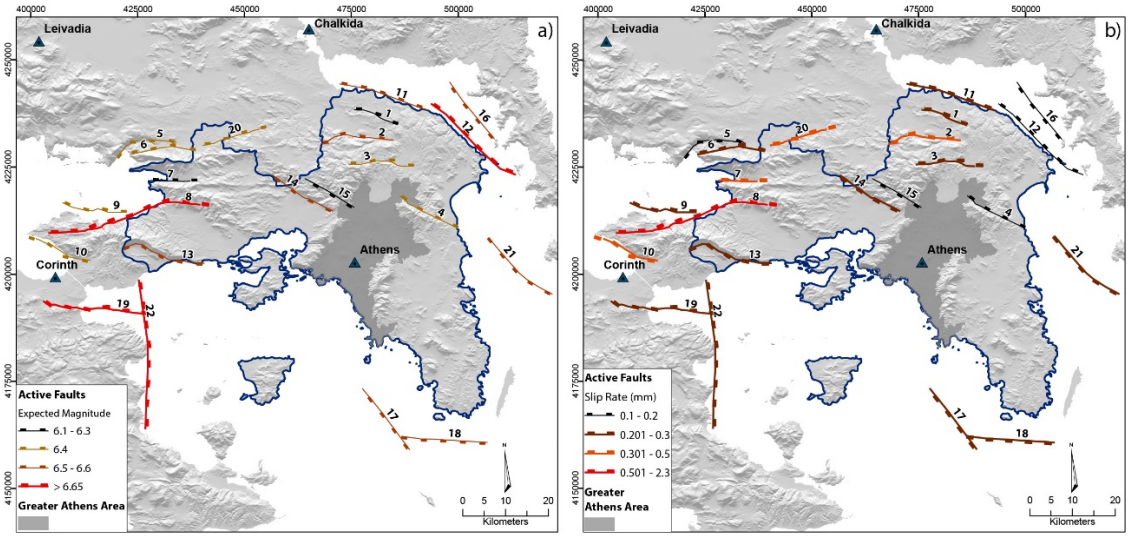

Figure 4: Map of active faults that can sustain damage within the region of Attica. a) Different colors represent the maximum expected magnitude that these faults can generate. b) Different colors represent different slip-rate categories. Slip rates govern earthquake recurrence. As slip rates increase, average earthquake recurrence intervals tend to decrease.

Table 3: Fault characteristics used for extracting the earthquake recurrence per site over the last 15 kyrs. Expected Magnitude and Maximum Displacement per Event values are based on Wells and Coppersmith (1994) equations. Slip rate column refers to short term where available, or long term slip rate values, induced from published papers and neotectonic maps (see text for details). *Id* numbers refer to the map displayed in Figure 1. Fault characteristics are based on the following sources (numbers correspond to the "Source" column): *1)* Official Neotectonic map Saronikos Gulf – Papanikolaou, et al. 1989a; *2)* Official Neotectonic map South Evoikos Gulf – Papanikolaou, et al. 1989b; *3)* Neotectonic map East Attica – Papanikolaou, et al. 1995; *4)*Pantosti, et al. 1996; *5)*Collier, et al. 1998; *6)*Morewood & Roberts, 1999; *7)*Morewood & Roberts, 2001; *8)*Pavlides, et al. 2002; *9)*Goldsworthy, et al. 2002; *10)*Benedetti, et al. 2003; *11)*Ganas, et al. 2004; *12)*Chatzipetros, et al. 2005; *13)*Ganas, et al. 2005; *14)*Kokkalas, et al. 2007; *15)*Papanikolaou & Papanikolaou, 2007; *16)*Sakellariou, et al. 2007; *17)*Rontoyianni & Marinos, 2008; *18)*Tsodoulos, et al. 2008; *19)*Roberts, et al. 2009; *20)*Roberts, et al. 2011 and *21)*Grutzner, et al. 2016. *f*: fieldwork findings.

Id	Length (km)	Postglacial Throw (m)	Expected Magnitude	Slip Rate (mm/y)	Maximum Displacement per Event (m)	Source
1	9.7	4.5	6.2	0.30	0.32	*9,15,21*
2	17.7	6.0	6.5	0.40	0.80	*9,11,13,15*
3	14.2	4.5	6.4	0.30	0.58	*15*
4	14.8	1.5	6.4	0.10	0.61	*15*
5	14.5	3.0	6.4	0.20	0.59	*10,14,18,19*
6	15.7	4.5	6.4	0.30	0.67	*f*
7	9.2	7.5	6.1	0.50	0.30	*f*
8	32.8	34.5	6.7	2.30	2.04	*4,5,7,19,20*
9	15.1	4.5	6.4	0.30	0.63	*16*
10	13.9	7.5	6.4	0.50	0.56	*20*
11	21.8	4.5	6.6	0.30	1.10	*15*
12	26.2	1.5	6.7	0.10	1.45	*2*
13	19.6	4.5	6.6	0.30	0.94	*13,17*
14	16.5	4.1	6.5	0.27	0.72	*8,13*
15	13.3	2.6	6.3	0.17	0.52	*8,13*
16	17.0	2.4	6.5	0.16	0.76	*2*
17	18.1	4.4	6.5	0.29	0.83	*1*
18	19.3	3.7	6.6	0.25	0.92	*1*
19	23.7	4.4	6.7	0.29	1.25	*20*
20	13.9	7.0	6.4	0.47	0.56	*f*
21	19.6	4.4	6.6	0.29	0.93	*2*
22	35.0	3.3	6.7	0.22	2.25	*1*

350

351 **3.2 Seismic Hazard Maps**

352 Four detailed seismic hazard maps were compiled for the region of Attica, one for
353 each of the intensities VII – X (MM). These maps offer a locality specific shaking

recurrence record, which represents the long-term shaking record in a more complete way than the historical/instrumental catalogue, since they incorporate several seismic cycles of the active faults that affect Attica (Figures 5 - 8).

3.2.1. Intensity X

Intensity X is mostly observed in limited areas in the hanging wall of large faults, covered by loose sediments (Figure 5). Surface geology plays the most important role for the intensity X occurrence, as it increases by a single value the calculated isoseismals of intensity IX that only larger faults can produce in case of seismic rupture. The highest recurrence of intensity X (>20 times in the past 15 kyrs) is observed only in the western part of Attica, close to the Corinth Gulf. This is attributable to the high slip rate value of the fault that was activated during the 1981 earthquake (South Alkyonides Fault system), which is capable of producing earthquakes of magnitude M = 6.7. A second peak (11 times in the past 15 kyrs) in recurrence is observed in the northern coastal zone (Oropos area). This area is affected by two large faults (faults n.2 and 11 on Table 3) and is also covered by loose alluvial and Plio – Pleistocene sediments. Large areas are expected to have been shaken in such intensities in the Thriassio plain, west of the Greater Athens Area, but their recurrence is relatively low, due to the low slip rates of the neighboring faults. It is important that no intensity X is expected for the Greater Athens Area, as it is located far away, or in the footwall of potentially damaging long faults (id = 2, 8, 11, 12, 14 on Table 3).

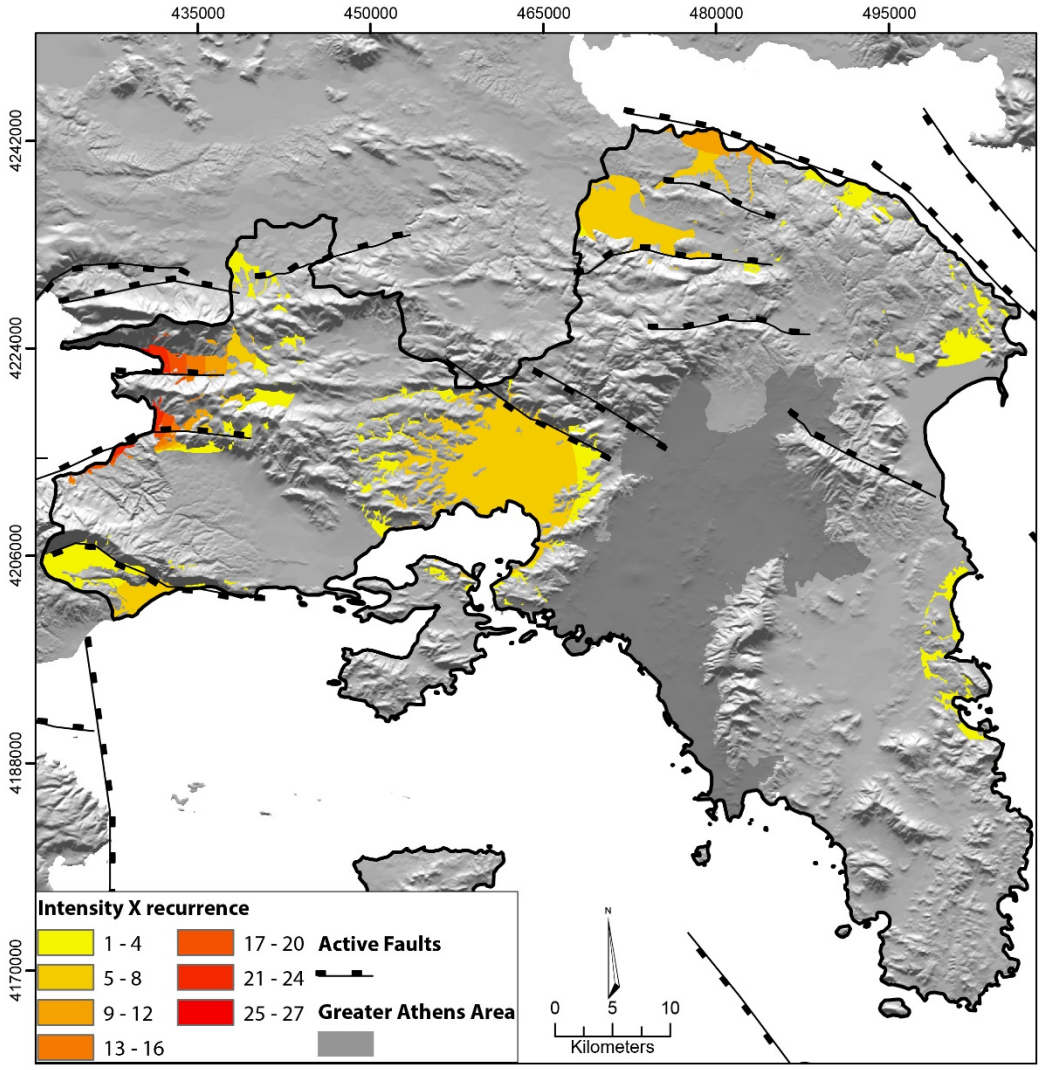

Figure 5: Seismic hazard map of Attica, showing the estimated site specific recurrence for intensities X (MM). The Greater Athens Area is not expected to have experienced such intensities during the last 15 kyrs.

3.2.2. Intensity IX

Intensity IX is expected to have occurred in larger areas of Attica and in higher recurrence levels, compared to intensity X (Figure 6). This is attributed to the fact that the calculated isoseismals of the shorter faults (< 16 km) are also taken into account in the modeling procedure. Intensity VIII isoseismals are amplified by one value when applied to loose sediments and are then added to the larger faults impact. Even though recurrence values are relatively low, it is important to note that intensity IX is

382 expected up to 11 times in the western parts of the Greater Athens Area and only 2
383 times in sparse areas in the eastern parts of the Athens plain. The loose alluvial
384 sediments of the Kifissos River which flows near the center of Athens, along with the
385 Upper Pliocene – Lower Pleistocene lake sediments at Chalandri and surrounding
386 areas (Papanikolaou, et al. 2004, localities shown in Figure 3) increase the intensity
387 values. Severe damages were inflicted during the Athens 1999 Mw 5.9 earthquake in
388 such geological formations (Lekkas, 2000). The highest recurrence (77 times, or
389 nearly 195 year return period) is observed in the western part of Attica, due to the
390 highly active South Alkyonides Fault. Moreover, the seismic hazard is also increased
391 close to the Saronic Gulf coastline, which is expected to experience intensity IX with
392 a minimum return period of 288 years. The northern part of Attica is mostly affected
393 by Afidnai, Avlonas – Malakasa, Milessi and Oropos faults (faults no. 3, 2, 1 and 11
394 in Table 3, respectively), which explains the relatively high intensity IX recurrence
395 (up to 37 times, or 405 year return period) that seems to have occurred since the last
396 glaciation.

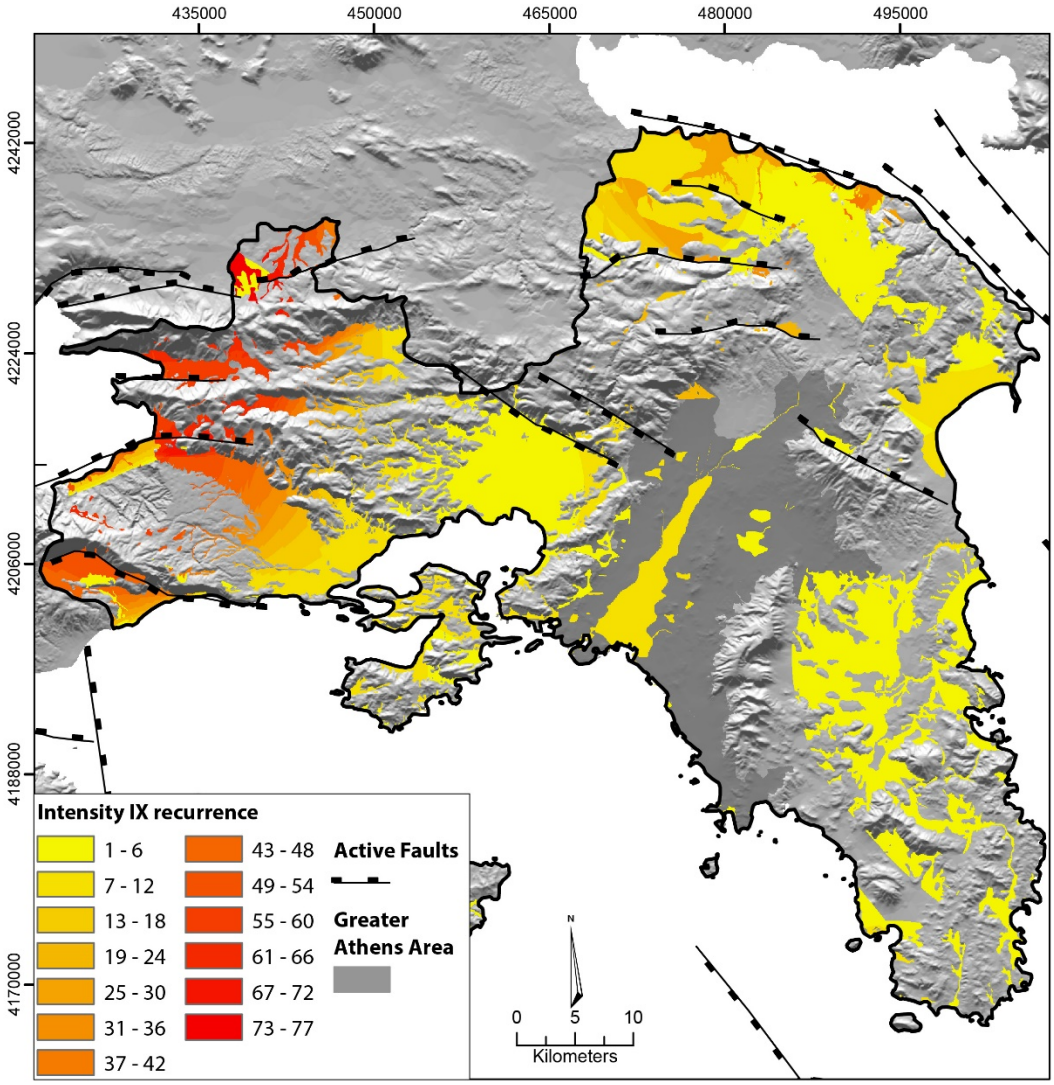

Figure 6: Seismic hazard map of Attica, showing the estimated site specific recurrence for intensities IX (MM).

However, as indicated also in the intensity X spatial distribution (Figure 5), it seems that the central Athens area has not experienced high intensities during the last 15 kyrs, which comes in agreement to Ambraseys and Psycharis (2012) conclusions for lack of evidence for destructive events in the ancient and historical old part of the town for the last 2300 years. Nevertheless, the expansion of the city through the last decades has increased both the vulnerability and the hazard in particular areas with poor geotechnical conditions.

3.2.3. Intensity VIII

405 Intensity VIII covers larger areas in the Attica mainland because of the larger
406 isoseismals for intensity VIII on the larger faults. As a result, there is also an increase
407 in intensity VIII recurrence in the Attica main land, compared to the intensities X and
408 IX (Figure 7). The highest recurrence, outreaching 100 the times over 15 kyrs, seems
409 to have occurred in the Megara basin, NW of Salamina island, mostly because this
410 area is now partly affected by the highly active South Alkyonides fault system, as
411 intensity VIII occurs in a distance between 11 and 25 km from the large faults (see
412 Table 1). Indeed, during the 1981 event, when this fault system ruptured, Megara
413 basin suffered serious damage (Ambraseys and Jackson, 1981; Antonaki,et al. 1988,
414 Papanikolaou, et al. 2009). Moreover, the majority of the central and the western part
415 of the Greater Athens Area seems to have experienced intensity VIII, 20 times during
416 the last 15 kyrs on average, due to the low slip rates of the faults that affect this part of
417 Attica.

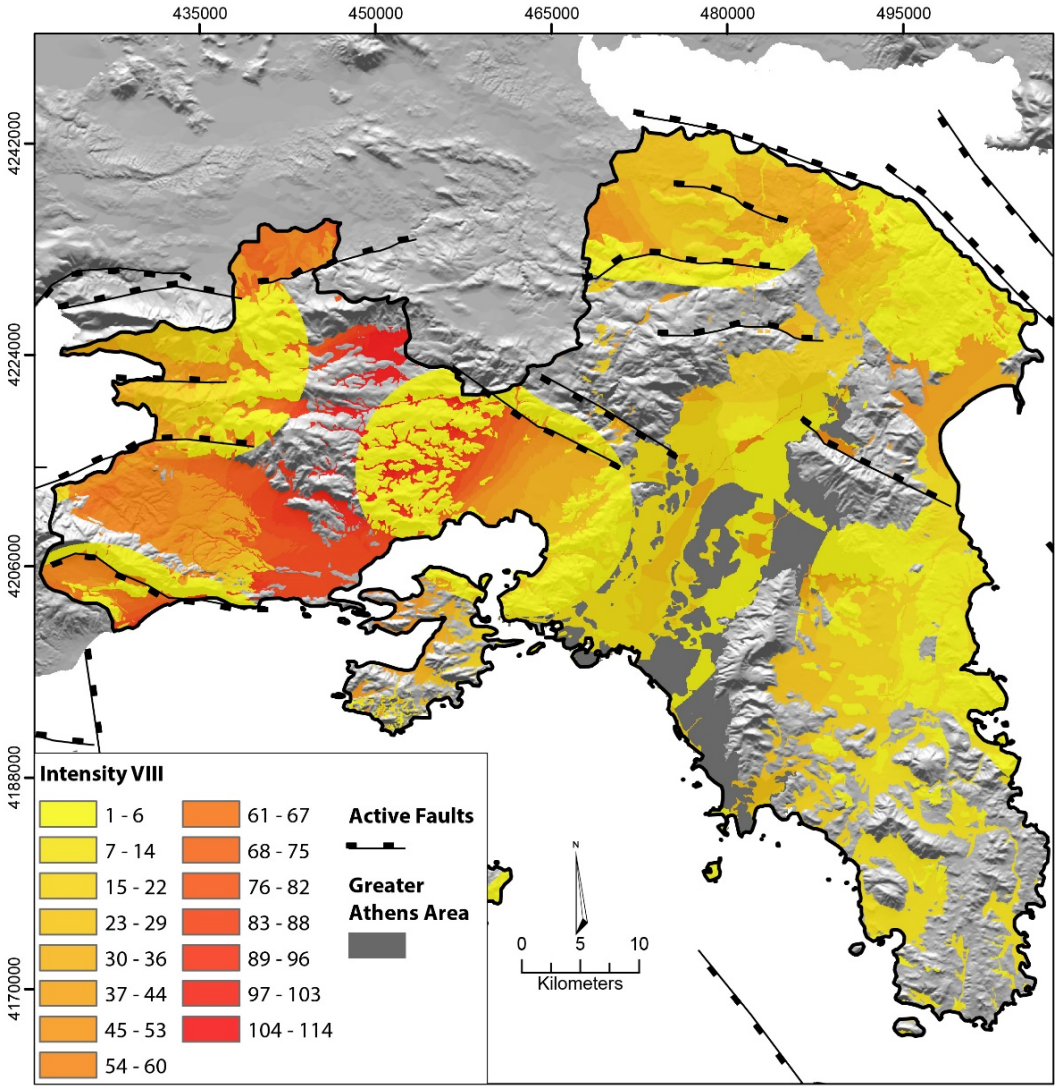

Figure 7: Seismic hazard map of Attica, showing the estimated site specific recurrence for intensities VIII (MM).

3.2.4. Intensity VII

Almost every part of the Attica mainland seems to have experienced intensity VII at least once during the last 15 kyrs, except for the Hymettus Mountain which seems to have not been shaken in intensity VII due to its bedrock geology (mostly marbles and schists) and its large distance from faults (Figure 8). Recurrence levels in the Attica mainland reach up to 150 times, mostly observed in the center of the Greater Athens Area in a NNE – SSW general direction. Even distant faults seem to affect this part of Attica which lies in the conjunction of the majority of the active faults' lower

intensities isoseismals. The seismic risk is increased in this area which is densely inhabited, although light industries and warehouses are also located mostly near the Kifissos River. It is noteworthy that during the Athens 1999 Mw 5.9 earthquake, severe and moderate damages were observed in the northern parts of the Kifissos riverbed, in a NNE – SSW general direction of the intensity contours (Lekkas, 2000).

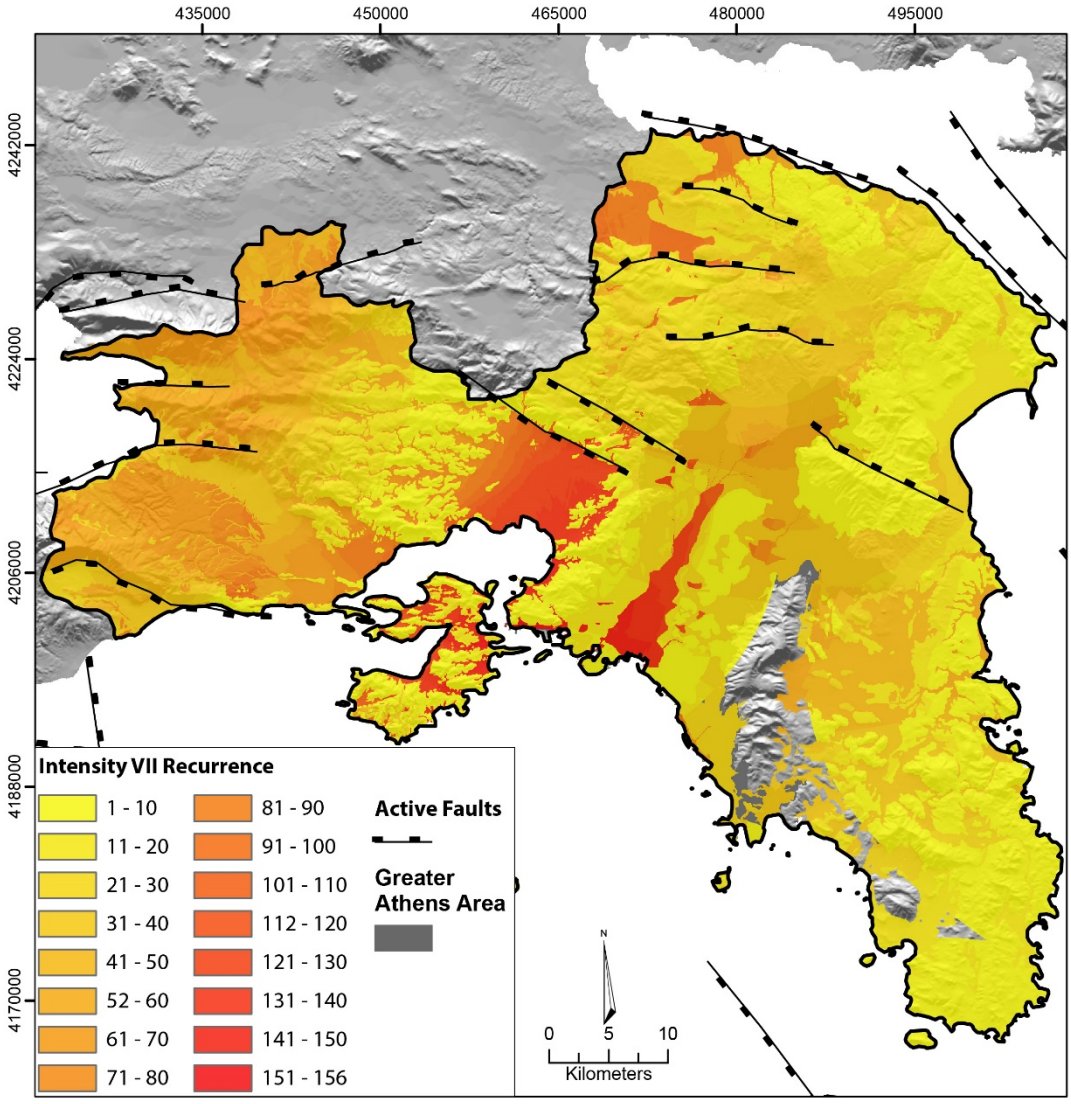

Figure 8: Seismic hazard map of Attica, showing the estimated site specific recurrence for intensities VII (MM). Nearly every suburb of the Greater Athens Area has experienced such intensities in the past 15 kyrs, including the recent 1981 earthquake sequence and the 1999 event.

3.2.5. Maximum expected intensity map

Figure 9a shows a combination of the intensities layers, providing information for the maximum expected intensities for each locality in Attica mainland. It is important to note that this map contains no information about the intensities recurrences. Instead, it displays the maximum ground motions that any locality seems to have experienced over 15 kyrs, even if they had occurred only once. As a result, this map is valuable for defining the worst case scenario in terms of the maximum ground motions expected.

Higher intensities (IX – X) are observed proximal to the large active faults, mostly in the northern and western parts of the Attica mainland. Intensity X seems to occur in areas covered by loose sediments that are close to major faults. Localities that are also covered by loose sediments but lie in a further distance from large faults or close to smaller faults, seem to have at least once been shaken at intensity IX. It is important to note that many localities in the Greater Athens Area seem to have received enough energy to shake at intensity IX over the last 15 kyrs. On the other hand, it seems that the largest part of the Greater Athens has not experienced destructive ground motions and the maximum expected intensities are VIII or VII.

3.2.6. Maximum recurrences distribution

The top quintile of the intensities VII – X recurrences is displayed in Figure 9b. This map shows the highest (top 20%) recurrences from each intensity and the corresponding spatial distribution in different colours. Thus, it depicts the locations where the peak recurrences of each intensities are observed, rather than the most hazardous areas in terms of maximum expected intensities. For example, the southern suburbs of the Greater Athens Area seem to have experienced intensity VII more

456 times than the rest of the Athens plain, however, this is not the maximum expected
457 intensity for this area.

458 The peak recurrences for every intensity are observed in the western part of the
459 Attica mainland. The top 20% intensity X recurrence (22-27 times over 15 kyrs) is
460 constrained in a small area, only along the loose sediments of the western Attica
461 coastline, in the Corinth Gulf, close to the highly active South Alkyonides fault
462 system. The highest intensity IX recurrence (62-77 times over 15 kyrs) is observed in
463 a wider area, in the westernmost parts of the Attica mainland. As intensities decrease,
464 their peak recurrences seem to move towards the center of Attica. Intensity VIII
465 seems to occur in its maximum recurrence (91-114 times over 15 kyrs) between the
466 Corinth and the Saronikos Gulfs, while the top 20% of the intensity VII recurrence is
467 observed in the eastern part of the Thriassio plain, the NW part of the Greater Athens
468 Area and Salamina Island in the Saronic Gulf. However, it is possible that the
469 distribution of the top 20% recurrences for intensities VIII and VII in the western part
470 of Attica is underestimated, because active faults located farther offshore in the
471 Corinth Gulf are not included in the model. Furthermore, fault specific seismic hazard
472 maps are able to model events of magnitude M>6.0 and as such they tend to
473 underestimate intensity VIII and predominantly intensity VII recurrence.

474 Apart from the South Alkyonides fault, it is evident that more faults contribute to the
475 total recurrence for intensities lower than X. As the intensities decrease, the
476 isoseismals increase and more faults contribute to seismic hazard. However, as
477 expected, the highest recurrences seem to be highly affected by the high slip rates of
478 the South Alkyonides fault.

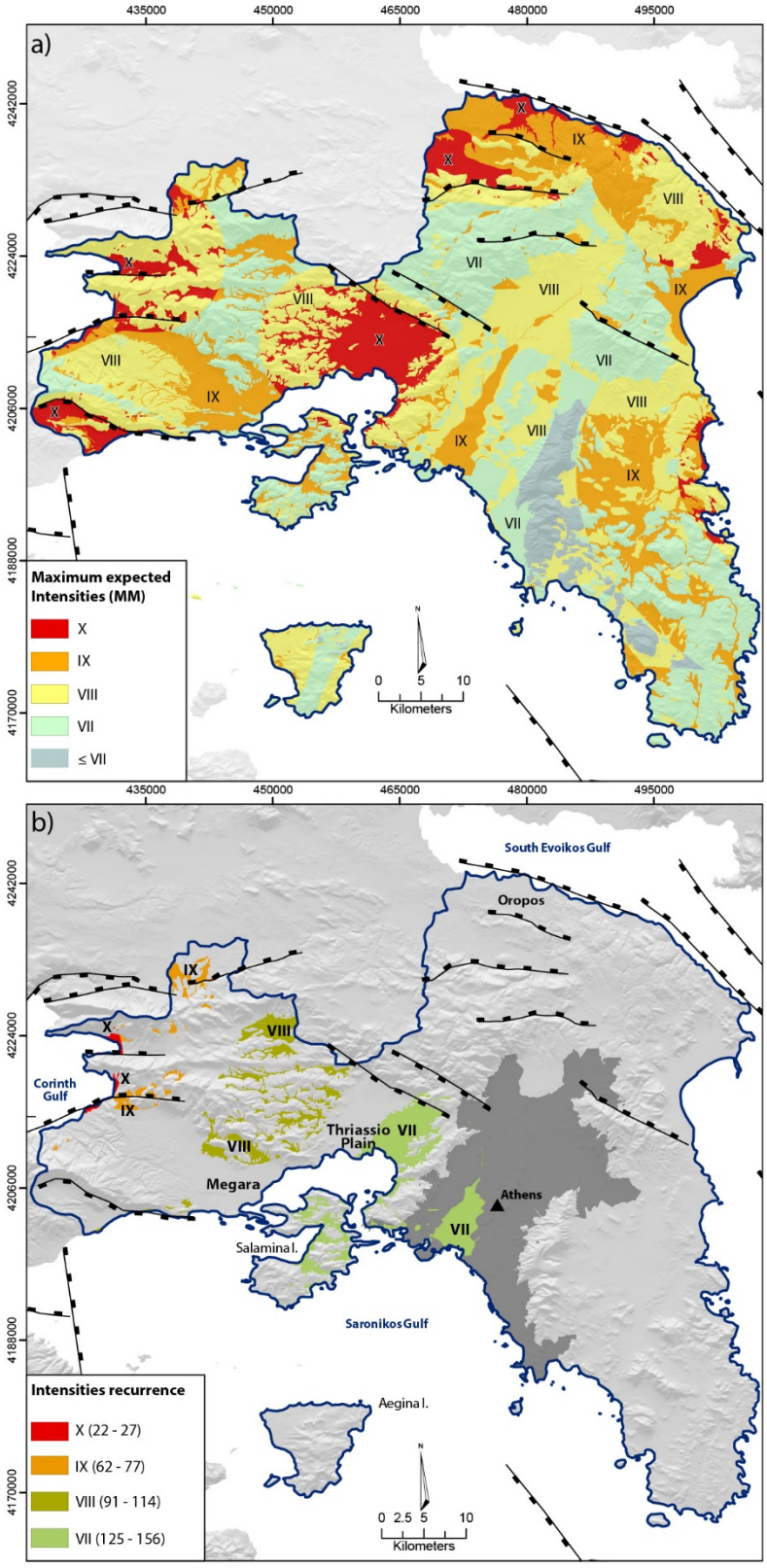

Figure 9: a) Maximum expected intensities distribution for each locality in the Attica mainland. b) the maximum intensity locations are defined by the proximity to the active faults and the surface geology Top quintile (top 20%) for the recurrences of the intensities VII – X.

The recurrence values in each locality of the fault specific hazard maps (Figures 5 - 8) can be used as input for calculating probabilities of strong ground shaking in high spatial resolution, over a certain time period. Since the historic seismic record is incomplete for the majority of the active faults, the stationary Poisson model can be utilized for the calculation of locality specific probabilities (see also Papanikolaou, et al. 2013) for each locality of the Attica mainland, based on the average recurrence intervals of the intensities VII - X. If λ is the rate of occurrence of certain seismic events within a time *t*, the probability that *n* events take place within such interval is: $Poisson = \frac{\lambda^n e^{-\lambda}}{n}$. If the occurrence of events follows a Poisson distribution, then the intervals of time t between consecutive events have an exponential distribution (Udias, 1999). In this case the equation for the probability density function is: $P(n) = \lambda e^{-\lambda \delta t}$, whereas the cumulative distribution function is $P = 1 - e^{-\lambda t}$ (Papoulis, 1991; Udias, 1999). This model is usually applied when no information other than the mean rate of earthquake production is known (WGCEP, 1999).

The high spatial resolution of the maps allows an assignment of the λ value in different scales, varying from building blocks, to Postal Code or Municipality level (e.g. in Figure 10). Using the Poisson model and the λ values derived from the intensities recurrence, a time-independent probability of shaking at intensities VII - X can be calculated for every desired area in the map, for a given time period.

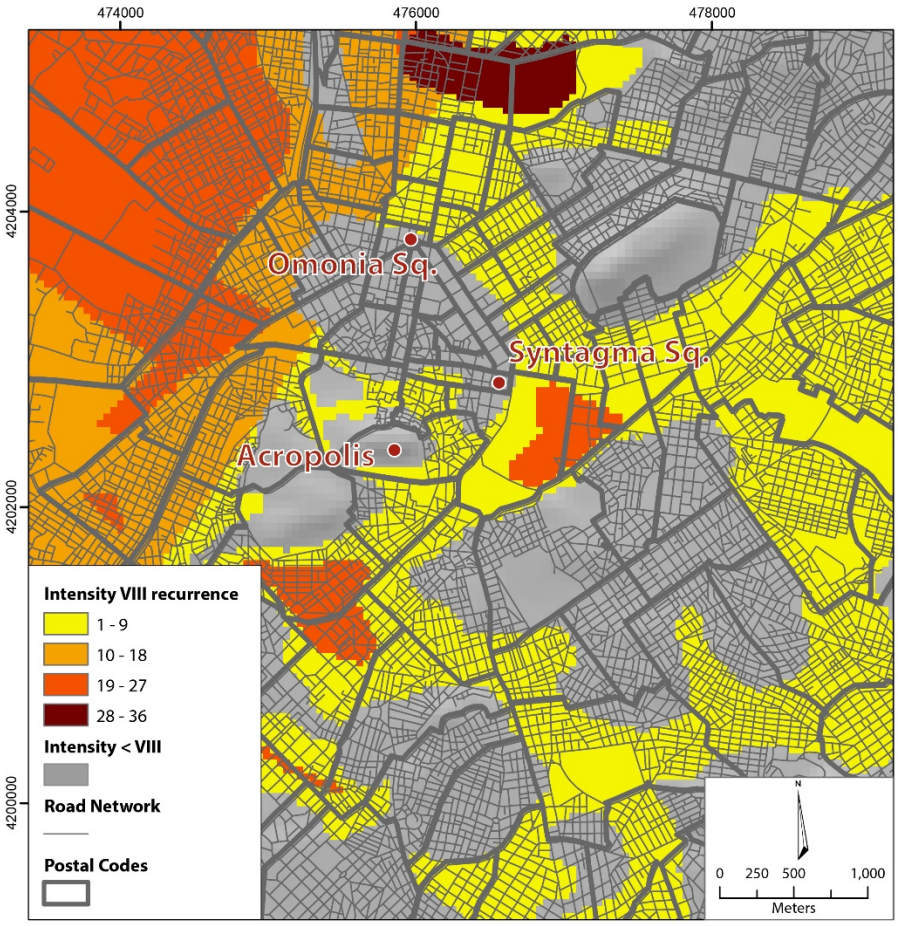

Figure 10: Fault Specific Seismic hazard map of the Athens center. Color variations show how many times these localities have received enough energy to shake at intensity VIII over the past 15kyrs. This map offers a high spatial resolution of the intensities' distribution and recurrence, therefore it allows a detailed calculation of λ values in Postal Code or even building block level.

4. Errors and major assumptions

Seismic hazard maps incorporate uncertainties as their predictions vary significantly, depending on the choice of many poorly known parameters (Stein, et al. 2012). The analysis of the active faults and the geologic conditions in the Attica mainland aims on reducing the major uncertainties attributed to the historic earthquake catalogues. However, assumptions made in key methodology aspects are connected to: a) faults

504 determination and fault geometry, b) fault slip rates, c) surface geology and d)
505 intensity attenuation relationships.

506 a) Both qualitative and quantitative assumptions were made for the delineation of
507 the fault database. The presented active faults are constrained in a way that
508 literature findings and personal fieldwork are in agreement to the tectonic activity
509 regime in Attica. Regarding fault lengths, the error parameters are well
510 communicated in the corresponding literature, where applicable (see Benedetti, et
511 al, 2003; Ganas, et al. 2005; Papanikolaou & Papanikolaou, 2007; Sakellariou, et
512 al. 2007; Roberts, et al. 2009; Grutzner, et al, 2016;). Faults lengths are estimated
513 around ±10%, whereas faults derived from neotectonic maps may also include a
514 spatial error of the order of ± 300 – 400m that can reach 500m (Ganas and
515 Athanassiou, 2000). Fieldwork findings were based on 1:50,000 geological maps
516 and crosschecked using slope maps, based on the 20m contours of topographic
517 maps with a nominal accuracy of 25m in the XY axes (Ganas and Athanassiou,
518 2000).

519 One of the major questions is whether all active faults have been traced and
520 included in the database. Considering that Attica is a well-studied area with major
521 infrastructure, all major active faults have been identified. However, four potential
522 active fault structures are not taken into account in the modeling procedure (see
523 faults P1 – P4 in Figure 11 for approximate locations). It is not clear whether these
524 are active structures, due to considerably unclear indications about their existence
525 and level of activity. Indications in neotectonic maps of East Attica (Papanikolaou,
526 et al. 1995) and the South Evoikos submarine neotectonic map (Papanikolaou, et
527 al. 1989b) are not clear about the existence and throw rate regarding the P1
528 probable fault. In fact, the neotectonic map of East Attica suggests that P1 is a

probably inactive structure, with an overall small amount of finite throw. It seems that P1 is a WNW – ESE trending structure, parallel to the Oropos fault, dipping towards the center of the South Evoikos Gulf. In addition, geomorphic and geologic signs about P2 and P3 faults suggest that these structures need further analysis. Antoniou (2010) argues that small faults like P2 (Figure 11) may act as active boundaries on the existing basins in east Attica. However, these structures were characterized by Papanikolaou, et al. (1995) as "mostly inactive". Regarding P3, there is some evidence for neotectonic activity, according to Mariolakos, et al. 2001 and Theocharis & Fountoulis, 2002. Moreover, this structure seems to be related to an offshore WNW – ESE trending fault zone with a noticeably small total throw, rupturing Mesozoic sedimentary rocks and Plio-Quaternary sediments (Papanikolaou, et al. 1989). Similarly, Papanikolaou, et al. (1998) describe the P4 fault in Aegina Island as a SW-NE trending structure. This fault seems to have an offshore prolongation with a small amount of throw in the northeastern submarine area (Papanikolaou et al. 1989) and forms small scarps throughout the sedimentary and volcanic formations in the surface of Aegina.

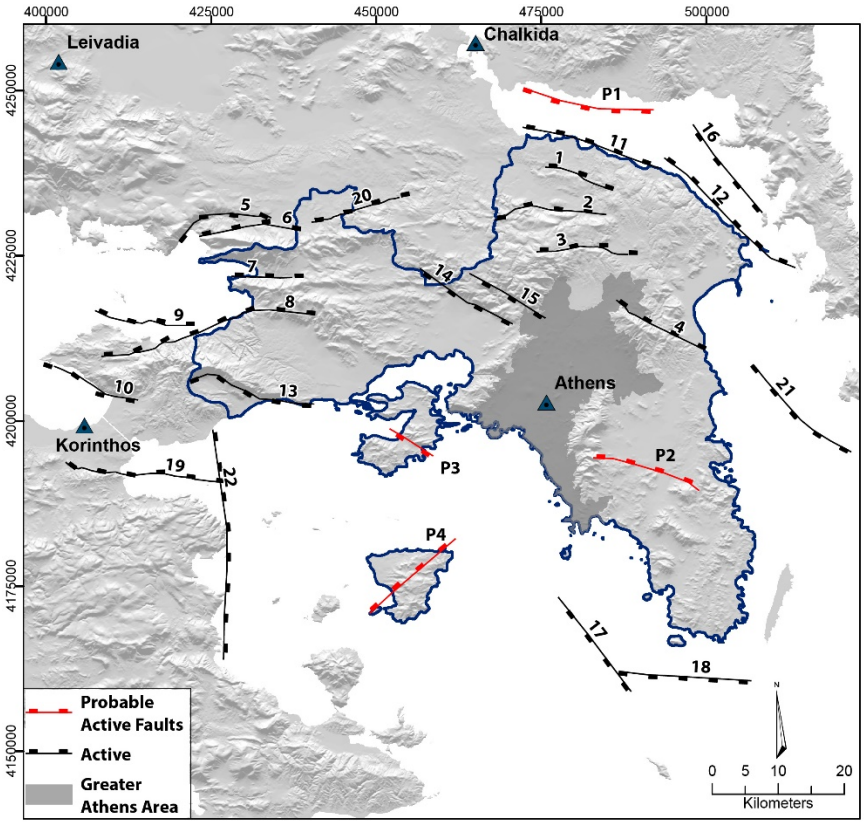

Figure 11: Probable active fault structures (red colour) in Attica region. These faults are not taken into account in seismic hazard mapping as they are either antithetic structures of major fault zones (northern part of Attica), or it is unclear whether they are active or not. In any case, their contribution to seismic hazard modeling is considerably lower than the already analyzed active structures.

Consequently, no significant changes would occur in the hazard maps if these faults had been included in the seismic hazard mapping of the Attica region, as their slip rate values would be less than 0.1mm/y, judging from their finite throw. This implies an earthquake recurrence of less than 3-4 times over 15 kyrs, making no considerable difference to the total recurrence values. However, since this is a GIS based methodology, new data or updated data on the already analyzed faults can be incorporated in seismic hazard scenarios, should any more information for these faults occur in the future.

It is also important to note that we chose to model only active faults that were capable of producing earthquakes of magnitude Ms > 6.0, with clear surface

555 ruptures. Indeed, earthquakes with magnitude Ms < 5.5 are unlikely to break the
556 surface (Michetti et al., 2000) and earthquakes of magnitude < Ms 6.0 are usually
557 poorly expressed at the surface, as discontinuous traces or fractures (e.g. Bonilla, et
558 al. 1984; Darragh & Bolt, 1987).
559 b) Fault slip rate values dominate the intensity recurrences of the fault specific
560 seismic hazard maps. It is of decisive importance that errors in slip rate
561 measurements are reduced in way that they do not affect the final earthquake
562 recurrence values. Already published slip rate values for active faults included
563 information about the error or minimum and maximum values (e.g. Ganas, et al.
564 2005). Both in this case, and in case of neotectonic maps, we used the average slip
565 rate values or the average finite throws and sediments thickness. The latter was
566 applied on faults derived from the official neotectonic maps. Since there is no
567 detailed information about the sediments thickness or the active faults total throw,
568 long term slip rate values were extracted by combining both values. Value ranges
569 for both sediments thickness and faults total throw have a maximum variation of
570 ±100m, which results to ±0.04 on long term fault slip rate values. Slip rate
571 characteristics for faults derived from fieldwork depended on errors in scarp height
572 measurements. A scarp height variation of ± 20% (see also Roberts, et al. 2004) is
573 assumed, which results to ± 0.2mm/y for a fault with a slip rate of 1mm/y.
574 c) Geological maps at 1:50,000 scale often include a standard error of ± 200 m.
575 1:100.000 scale neotectonic maps exceed ± 400 m spatial error (Ganas and
576 Athanassiou, 2000). Except for the exact fault location and length, these
577 uncertainties affect the accuracy of the spatial distribution of the strong ground
578 motions, since surface geology amplifies or attenuates the calculated intensities.
579 For the spatial distribution of the modeled intensities we used the official 1:50,000

Geological Maps of IGME and the 1:25,000 map of E.P.P.O. (Marinos, et al. 1999). These maps provide an adequate spatial analysis regarding surface geology and the corresponding attenuation or amplification of the strong ground motion. Furthermore, they can offer critical information about earthquake-induced secondary effects, such as landslides and liquefactions.

d) Expected intensity at certain localities is highly sensitive to the relationships that calculate the attenuation of strong ground motion with distance from the epicenter. Final results can be drastically affected by the uncertainties incorporated in the fault geometry (and thus in the epicenters location) and in the attenuation relationships that are based in the traditional intensity scales. For example, Papanikolaou (2011) quantified errors in both spatial distribution and recurrence intervals of the expected intensities in the Apennines and showed that they can outreach the aforementioned 20% error of the fault slip rates, modifying the estimated recurrence intervals by as low as 10-25% and as high as 1000%. Therefore, the attenuation relationships used, form a major source of uncertainty and in several cases they overshadow all the other factors of uncertainty, even fault slip-rates, which directly affect the calculated earthquake recurrences.

5. Discussion

5.1 Uncertainties in intensity distribution

The largest uncertainty in seismic hazard mapping lies on the attenuation relationships, based on the traditional intensity scales. From a point of view, this is an inevitable assumption that has to be made when intending to examine damages in the built environment. On the other hand, Earthquake Environmental Effects (EEE) are

603 objective criteria indicating the severity or ground shaking in the non-built
604 environment. Since they are not influenced by human parameters, they overstep
605 problems that are inherited in traditional intensity scales, which tend to reflect mainly
606 the economic development and the cultural setting of the area that experienced the
607 earthquake, instead of its "strength" (Serva, 1994). The Environmental Intensity Scale
608 - ESI 2007 (Michetti, et al. 2007) incorporates the advantages of Earthquake Geology
609 and uses EEE for the determination of seismic intensity (Michetti, et al. 2007;
610 Reicherter, et al. 2008; Silva, et al. 2009). Moreover, it can define the intensities
611 above VII degree with a high level of accuracy as also shown in several recent and
612 historic earthquakes worldwide (e.g. Serva, et al. 2007; Tatevosian, 2007;
613 Papanikolaou, et al. 2009). New attenuation relationships for the ESI 2007 intensity
614 scale, would remarkably reduce the error incorporated in the existing seismic hazard
615 maps. Papanikolaou, et al. 2009 implemented the ESI 2007 intensity scale for the
616 1981 Alkyonides earthquake sequence in the Corinth Gulf (Ms = 6.7, Ms = 6.4, Ms
617 =6.3) and showed that it allows accurate assessment on sparsely populated areas. This
618 implies that ESI 2007 could be used outside of the Greater Athens Area for modeling
619 the ground shaking distribution in a higher accuracy than the traditional intensity
620 scales.

621 The implementation of the topographic amplification factor in the modeling
622 procedure, as described in Eurocode 8 for the European Union (Bisch, et al. 2011),
623 could potentially increase the accuracy on the intensity distribution in the final
624 seismic hazard maps. This factor incorporates slope instability effects, usually
625 observed on isolated cliffs and ridges with crests and can be applied on Seismic
626 Hazard Analysis based on Peak Ground Acceleration (PGA) values (values are
627 multiplied by 1.2 to 1.4). However, according to Wald, et al. (1999) and Paolucci

628 (2002), an increase of PGA by a factor ranging from 1.2 to 1.4, implies an increase of
629 MMI ranging from 0.29 to 0.53, which is less than the increase (or decrease) derived
630 from the incorporation of geological conditions. Furthermore, we performed a test
631 regarding the impact of the topographic gradient in the Greater Athens Area. The test
632 showed that less than 0.4km^2 of inhabited areas (or ~ 0.1% of the Greater Athens
633 Area) meet the anaglyph parameters for the application of the topographic
634 amplification factor, thus the final maps would have imperceptible changes. This
635 parameter can be incorporated in more detailed microzonation studies.

636 **5.2 Historical seismic record compared to geological fault slip data**

637 The analysis of the active faults that can sustain damage (intensities ≥VII on the
638 Modified Mercalli intensity scale) in the Attica region in case of seismic rupture, aims
639 on addressing the problems related to the incompleteness of the historical records,
640 since geological data sample much greater periods of time. The historical seismic
641 record can be used for the seismic hazard analysis where smaller or blind faults can
642 cause moderate earthquakes up to magnitude 6, with potentially damaging effects in
643 older buildings. It is clear though, that the official seismic zonation in Greece
644 (E.P.P.O.) is based only on the historical earthquake catalogue and does not consider
645 a fault specific approach.

646 Despite the inconsistencies and inhomogeneity in historic earthquake catalogues, the
647 majority of the recorded events lie in the hanging wall of the hereby modelled active
648 faults. Among them, there are few recorded strong events that could cause
649 considerable damage, especially in the eastern part of the Attica Region (Figure 12).
650 However, large uncertainties regarding the position of the instrumentally recorded
651 epicenters are evident even for recent earthquake events. For example, the most

652 recent 1999 Mw 5.9 is recorded in both NOA-UOA (National Observatory of Athens
653 – University of Athens) and AUTH (Aristotle University of Thessaloniki) catalogues,
654 but the epicentral localities lay more than 5km apart. This uncertainty is magnified
655 more than two times for the 1938 Mw 6.0 Oropos event, where the distance between
656 the epicenters from these two catalogues is 12km. suggest that the errors on the
657 location of the instrumentally recorded epicenters can reach up to 20 km for the older
658 events (1965-1980) and up to 10km for the most recent ones. Larger uncertainties
659 result for the older events approximate epicentral locations. For the period 1901-1964
660 the errors can be up to 30km but they can reach up to 50km for the older events
661 (before 1900) when the number of available macroseismic information is less than 5.
662 Stucchi, et al. (2012) also observe uncertainties larger than 50km for regional
663 catalogues that cover the time window 1000 – 1899 in the Broad Aegean area.
664 Regarding the errors in magnitude, Papazachos, et al. (2000) suggest a ± 0.25 interval
665 for the instrumental period (1911-1999).They also attribute an ± 0.35 error for the
666 historical data, when the number of available macroseismic observations (number of
667 places where the intensity is known) is ≥ 10, otherwise the magnitude errors reach up
668 to a half of the magnitude unit. Furthermore, focal depths are not available for many
669 events recorded in the historic earthquake catalogues, thus there is a strong possibility
670 that many of the epicenters displayed in Figure 12 are actually attributed to the
671 subduction zone. Regarding the total number of historic earthquake events, there
672 seems to be no consistency, as there are events that don't exist in both catalogues.

673 In total, 9 events affecting the Attica region could be related to the analyzed faults.
674 Large uncertainties occur for 5 of them, as there are large variabilities regarding their
675 location and depth. On the contrary, 4 major events can be related to specific faults
676 with lower uncertainties. The 1981 Alkyonides earthquake sequence in the Corinth

677 Gulf (Ms = 6.7, Ms = 6.4, Ms = 6.3) can be attributed to South Alkyonides and
678 Kapareli faults (id No 5 and 8 in Table 3) (Jackson, et al. 1982). Moreover, the 1938
679 Oropos event (Ms = 6.0) could have probably ruptured the Oropos offshore fault (id
680 No 11 in Table 3, see also Papanikolaou and Papanikolaou (2007)), causing
681 considerable damage in the north part of Attika (Ambraseys and Jackson, 1990).
682 Other events, like 1705 (Figure 12b) have large uncertainties in their location, or even
683 are not included in both catalogues. For example, Papadopoulos, et al. (2002) argue
684 that the 1705 event could be located at a distance of about 30 km from the center of
685 Athens; however, the little macroseismic information available makes their epicentral
686 locations very uncertain. Ambraseys and Jackson (1997) fitted significant damage in
687 Athens and to the north of the town to the 1705 event, while for other events there
688 were no clear reports for serious damage in Athens or in other areas in Attica.

689 Eventually, 4 major events can be attributed to the fault database, suggesting that:

690 a) Due to low slip rates, the majority of the active faults may have not ruptured
691 during the last 200 or 500 years, which is the time period when historic seismic
692 catalogues are considered to be complete for earthquakes of M≥6.5 and M≥7.3
693 respectively.

694 b) There is a lack of resolution in the historic earthquake catalogues, as the number
695 of significant earthquake events is limited.

696 As a result, there is an overall spatial concurrence between the fault database and the
697 existing earthquake catalogues, for recent earthquake events. On the other hand, the
698 historic earthquake catalogues are inadequate for displaying the full extent of seismic
699 hazard, due to the lack of temporal and spatial resolution.

700 The large differences between the two catalogues shown in Figure 12 also indicate
701 that the information for recorded earthquakes, even for the most recent events like the
702 Athens 1999 earthquake, is not consistent. Thus, the association of the recorded
703 events to the known active faults need verification through further
704 palaeoseismological research.

705 **5.3 The role of the Miocene detachment in fault activity and intensities**
706 **distribution**

707 A major, now inactive, NNE-SSW striking fault system characterizes the geological
708 structure of Attica. It trends northeast and separates metamorphic rocks to the south
709 (Cycladic and Attica units) from non-metamorphosed units of the internal Hellenides
710 to the north (Papanikolaou and Royden, 2007). Although this zone acted during the
711 early and late Miocene time (Papanikolaou and Royden, 2007), it causes significant
712 local variations of strain rates. The southeastern part of Athens plain seems to be
713 under minor deformation rates, in contrast to the northwestern part, where higher
714 strain rates are observed, indicating the control of the inactive detachment on the
715 current deformation field of the region (Foumelis, et al. 2013). Moreover, this
716 detachment separates the E-W trending faults towards the western part of Attica, from
717 the NW-SE trending less active faults towards the eastern part (Papanikolaou and
718 Papanikolaou, 2007). The seismicity pattern is also influenced by the detachment, as
719 it coincides with the line that separates zone I (lowest category of seismic risk) from
720 zone II (intermediate zone) of the national seismic building code (EAK-2003, see
721 Figure 11), which has been compiled based on the seismicity level (Papanikolaou and
722 Papanikolaou, 2007).

723 Eastern Attica (the area east of the zone) lies mostly on metamorphic rocks, such as
724 marbles and schists that compose a massive, westward-dipping body. The area west of
725 the detachment (Western Attica) is mainly comprised of sedimentary rocks, such as
726 limestones and clastic formations. Recent post-alpine sediments, such as talus cones
727 and scree, that cover areas of lower altitude or even the slopes of the mountain fronts,
728 are often being used as the commonest foundation soils for urban structure (Lekkas,
729 2000).

730 Apart from the significant effect of the Miocene detachment on the neotectonic
731 structure of Attica, influencing the geometry, style and intensity of deformation
732 (Papanikolaou and Papanikolaou, 2007), it seems to have played a fundamental role in
733 the intensities distribution in case of earthquake events. During the Athens 1999
734 Mw=5.9 earthquake, the distribution of the strong ground motions and the heavy
735 building damages were concentrated in NNE-SSW oriented zones. These zones
736 coincide with or are parallel to the Miocene detachment, which seems to have
737 performed passively from the coastline of the Greater Athens Area, up to its
738 northernmost borders. High intensities, that were restricted in the areas west of the
739 detachment, were abruptly blocked and didn't enter the eastern suburbs
740 (Papanikolaou, et al. 1999; Marinos, et al. 1999b; Lekkas, 2000).

741 In this study, two parameters attributed to the effects of the detachment influenced
742 the intensities distribution. The first has to do with the different fault orientation and
743 activity on either sides of the detachment. Higher intensities and recurrence values are
744 observed in the western parts of the Attica mainland (see also Figures 5 and 6), due to
745 higher fault slip rate values. On the contrary, they lower intensities seem to affect the
746 eastern part of the Greater Athens Area or even the easternmost parts of Attica. The
747 second has to do with the loose sediments along the Kifissos riverbed, that flows

parallel and near to the detachment. This part of Attica seems to have been shaken several times at intensities from VII to IX (see also Figures 6-8) while the intensities distribution are in agreement whith the observed values during the Athens 1999 earthquake event.

5.4 Comparison with existing macroseismic intensity data from historic earthquake events

The difficulties and constraints on the comparison of the results with the available macroseismic data lie on two major factors. Firstly, the deficiencies in spatial resolution of the macroseismic intensity, especially for past events, affect the comparison regarding the intensities distribution. Secondly, the incompletence of the existing earthquake catalogues makes it difficult to compare the recurrence values over large periods of time, even for lower intensities (VIII or VII). Moreover, fault specific seismic hazard maps are able to model events of magnitude M>6.0 and as such they tend to underestimate intensity VIII and predominantly intensity VII recurrence. Indeed, events of lower magnitude are associated to the background seismicity and can sustain moderate damage in a limited area. However, they can't produce intensities as high as IX on the Modified Mercalli Scale. Also it is possible that the fault specific based recurrences for intensities VIII and VII in the western part of Attica are underestimated, because active faults located farther offshore in the Corinth Gulf are not included in the model. In any case, there could be a comparison of the fault specific seismic hazard maps with the existing descriptions of the damages distributions for recent earthquake events.

Four earthquake events affecting parts of the Attica region are recent enough to provide data for macroseismic intensity distributions. The 1938 Mw 6.0 Oropos is

772 reported as an intensity VIII (MM) event in areas close to the epicentre, at Northern
773 Attica (Ambraseys and Jackson, 1990). The central and southern parts, including
774 Athens, experienced lower intensities (VI) during the same event. During the
775 February Alkyonides earthquake sequence in the Corinth Gulf (Ms = 6.7, Ms = 6.4),
776 intensity VIII occurred in the town of Megara at the western parts of Attica, while the
777 Greater Athens Area experienced similar or lower intensities (VIII – VII). During the
778 March 1981 event (Ms = 6.3), intensity VII occurred near the Greater Athens Area
779 (Antonaki, et al. 1988). A more detailed picture of the intensities distribution during
780 the Athens 1999 Mw 5.9 earthquake is available by Lekkas (2000). He shows that the
781 highest intensity values (VIII – IX) are observed in a limited zone over the northern
782 parts of the Kifissos River sediments, mostly in NNE-SSW orientation. These areas fit
783 well to the ones that are shown to have experienced maximum intensities of VIII – IX
784 in Figure 9a. Although the observed intensities were recorded using the E.M.S.-1998
785 scale, they were directly converted to the MM Intensity scale for comparison
786 purposes, according to Musson, et al. (2010).

787 Regarding the recurrence values, the historic earthquake catalogues are considered
788 complete for less than 200 years for such events. However, based on these historic
789 events, a minimum return period of 100 years is observed for intensity VII in the
790 Greater Athens Area and for intensity VIII in the western parts of Attica. A minimum
791 200 years return period is observed for intensity VIII in the northern Attica and in
792 limited zones in the Greater Athens Area. Intensity IX is also observed in sparse
793 locations in the Greater Athens Area and in the westernmost parts of Attica mainland.
794 The findings for intensity VII in Athens agree with Papaioannou and Papazachos
795 (2000), who suggest that this area shakes at such intensities every 110 years.

However, there is a large difference for intensity VIII, as they suggest that the return period outreaches 1000 years.

Based on the fault specific seismic hazard maps, the same localities that experienced intensity VII during the 1981 series of 3 earthquakes (February - March) and the 1999 event show a return period from 200 years (western Attica) and 170 years (Megara), to 106 years (central part of the Attica plain, see also Figure 8). For the areas that have experienced intensity VIII during the February – March events, the return periods vary from 240 years in the western part of Attica, to more than 280 years in the central part and 440 years for the northern part of Attica (Figure 9a). Intensity IX seems to have a return period that varies from 714 to 1360 years in the same areas that were shaken in such intensities during the 1999 earthquake event and as low as 230 years for the westernmost part of Attica. Despite the fact that intensities VII and VIII are underestimated in the fault specific seismic hazard maps (see also Chapter 3.2.6), there is an agreement with the findings of Papaioannou and Papazachos (2000) for the recurrence of intensity VII in Athens. However, there is a large difference on higher intensities, as they suggest a 1000 year return period of intensity VIII in Athens, which is more than double comparing to the results of the fault specific hazard maps in most localities of the Greater Athens Area.

The differences between the historic catalogues and the seismic hazard maps based on geologic data indicate the need for longer observation time periods and higher spatial resolution in seismic hazard assessment.

5.5 Technical constraints on GIS processes

Seismic hazard mapping is primarily based on the perception of the spatial distribution of hazard. Final products, such as high spatial resolution seismic hazard

820 maps, are developed under complex GIS techniques. In this study we developed a GIS
821 database for the active faults characteristics, which also allowed us to apply various
822 GIS tools and techniques for the creation of the seismic hazard maps. We used
823 relative positions along the linear fault objects to store the geographic locations of the
824 earthquake distribution along strike each active fault line and from that point, we
825 automated the whole procedure in order to simplify the whole mapping process.
826 Existing tools were combined in order to develop a new powerful tool that
827 significantly reduces the time and inherent complexity in spatial analysis techniques,
828 allowing a consistent reproduction of the desired map outcomes. Moreover,
829 modifications regarding faults' activity, attenuation relationships and surface geology
830 can be easily implemented, while a full overview of the errors and assumptions
831 incorporated in seismic hazard mapping is possible. In any case, the accuracy of the
832 final maps depends on the main errors and assumptions already mentioned.
833

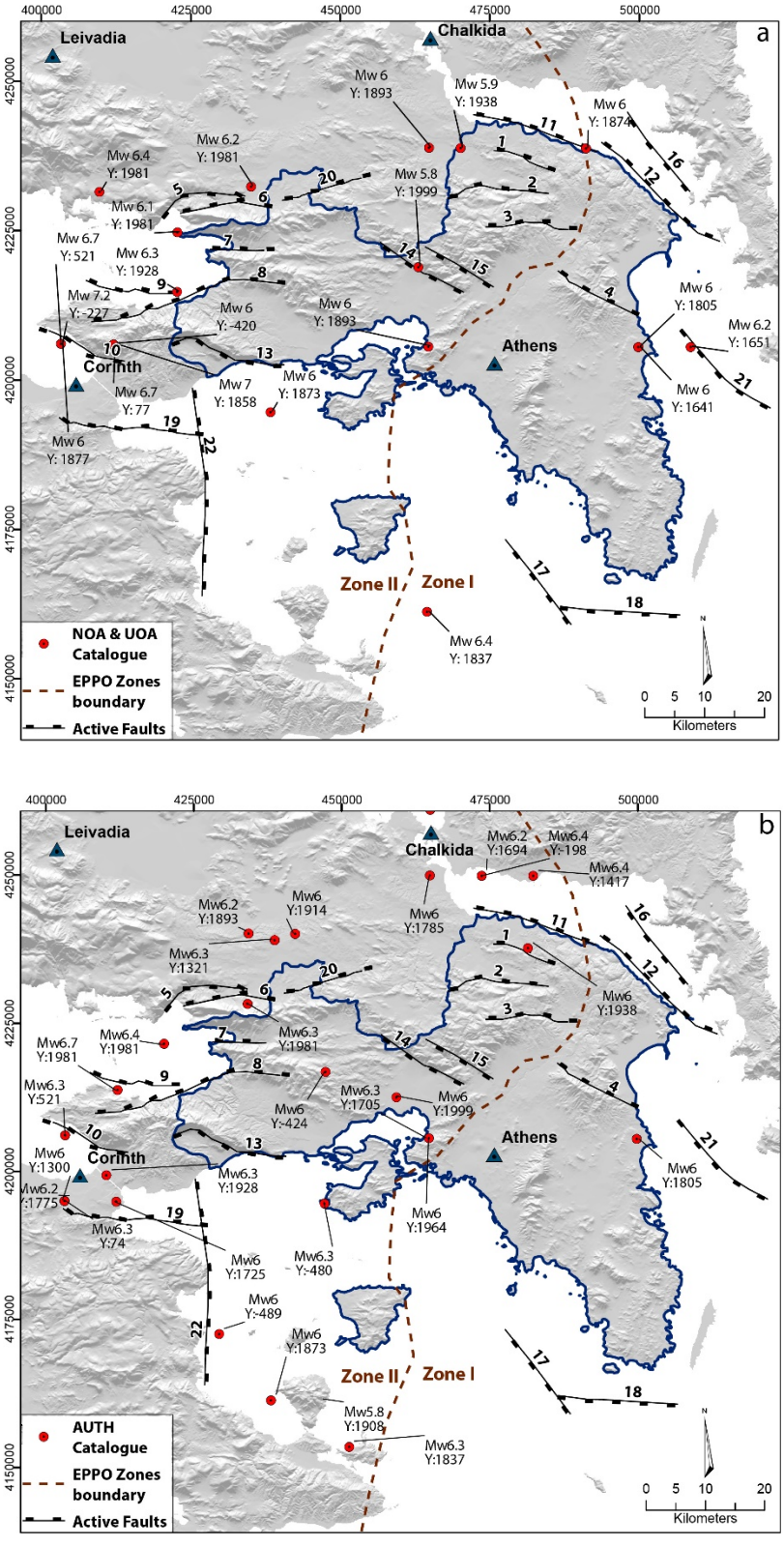

Figure 12: Historical earthquake record from a) the National Observatory and University of Athens (NOA&UOA) and b) the Aristotle University of Thessaloniki, for shallow earthquakes of magnitudes Mw>6 in comparison to active faulting in the Attica Region. The Athens 1999 and Oropos 1938 events are displayed in the NOA& UOA catalogue, although they are recorded as Mw5.8 and Mw5.9 events respectively. Focal depths are not available for the majority of the events in both catalogues, thus events with focal depth >20km might be also displayed. Both catalogues are

6. Conclusions

Four high spatial resolution seismic hazard maps have been developed for the region of Attica. These maps display both the spatial distribution and the recurrence, over 15 kyrs, of the intensities VII – X (MM intensity scale). They are based on a database of 22 active faults that could affect Attica region in case of seismic rupture. The majority of these faults have relatively low slip rates and the Greater Athens Area lies mostly on the active faults footwall. The spatial distribution of hazard depends on soil conditions for intensities X and IX and is governed by the distance from faults for intensities VIII and VII.

The Attica mainland seems to have been exposed to intensity X for more than 20 times in the last 15 kyrs, along the west coastline, in Corinth Gulf. Intensity IX is expected to have occurred up to 77 times over 15 kyrs in the westernmost parts of the Attica mainland. The highest recurrences for intensity VIII (114 times over 15 kyrs) are expected between the Corinth and the Saronikos Gulfs. The eastern part of the Thriassio plain, the NW part of the Greater Athens Area and Salamina Island in the Saronikos Gulf seem to have experienced intensity VII for up to 156 times over 15 kyrs. Large residential districts, even in the Greater Athens Area, have been shaken in high intensities (VIII – IX) for at least 10 times in the last 15 kyrs. In particular, intensity IX distribution is significant in the western parts of the Greater Athens Area and in sparse places in the eastern parts of the Athens plain. This is attributed to the loose alluvial sediments of Kifissos River, along with Upper Pliocene lake sediments at Chalandri and surrounding areas. Intensity VIII distribution depends both on large and small faults, so an increase of recurrence values (over 100 times in the last 15 kyrs in the western parts) is observed in Attica main land, compared to intensities X and IX. Almost every part of the Attica mainland seems to have experienced intensity

VII at least once during the last 15 kyrs. Recurrence levels reach up to 150 times, and are mostly observed in the center of the Greater Athens Area in a NNE – SSW general direction. Overall, the maximum expected intensities appear in the northern and western parts of Attica in high recurrences. On the other hand, the eastern part of Attica is possessed mostly by lower intensities, in low recurrences.

Regarding the seismicity record, there is an overall spatial concurrence between the fault database and the existing earthquake catalogues, for recent earthquake events. On the other hand, the historic earthquake catalogues are inadequate for displaying the full extent of seismic hazard, due to the lack of temporal resolution, highlighting the necessity for fault specific seismic hazard assessment.

Aknowledgements

The Antonios Papadakis scholarship from the National and Kapodistrian University of Athens is thanked for the support. Reviews from both referees strongly improved the paper.

7. References

Ambraseys, N.N., and Jackson, J.A., 1981. Earthquake hazard and vulnerability in the northeastern Mediterranean: the Corinth earthquake sequence of February-March 1981. Disasters 5(4), pp. 355-368.

Ambraseys, N.N., and Jackson, J.A., 1990. Seismicity and associated strain of central Greece between 1890 and 1988. Geophysical Journal International 101, pp.663-708.

Ambraseys, N.N., and Jackson, J.A., 1997. Seismicity and associated strain in the Gulf of Korinth (Greece) since 1694. Journal of Earthquake Engineering, 1(3), pp.433-474.

Ambraseys, N.N., and Psycharis, I.N., 2012. Assessment of the long-term seismicity of Athens from two classical columns. Bulletin of Earthquake Engineering 10, pp.1635-1666.

Antonaki, R., Vlachos, I., Staurakakis, G., Taflamba I., Tokas, Chatziandreou, S., Smpokos, I., Karydis, P., and Kaleuras, B., 1988. Earthquake economic impact – Insurance. Report in Earthquake Planning and Protection Organization (in Greek) 233pp.

Benedetti, L., Finkel, R., King, G., Armijo, R., Papanastassiou, D., Ryerson, F.J., Flerit, F., Farber, D., and Stavrakakis, G., 2003. Motion on the Kaparelli fault (Greece) prior to the 1981 earthquake sequence determined from ^{36}Cl cosmogenic dating. Terra Nova 15, pp.118–124.

896 Bisch P., Carvalho, E., Degee, H., Fajfar, P., Fardis, M., Franchin, P., Kreslin, M.,
897 Pecker, A., Pinto, P., Plumier, A., Somja, H., and G. Tsionis, 2012. Eurocode 8:
898 Seismic Design of Buildings Worked examples. In: B. Acun, A. Athanasopoulou,
899 A. Pinto, E. Carvalho, M. Fardis (eds). JRC Scientific and Technical Reports,
900 Luxembourg: Publications Office of the European Union.

901 Boncio, P., G. Lavecchia and B. Pace (2004). Defining a model of 3D seismogenic
902 sources for seismic hazard assessment applications: the case of central Apennines
903 (Italy). Journal of Seismology 8, pp. 407-425.

904 Bonilla, M.G., Mark, R.K., Lienkaemper, X., 1984. Statistical relations among
905 earthquake magnitude, surface rupture length, and surface fault displacement.
906 Bulletin of the Seismological Society of America 68, pp. 411–428.

907 Bornovas, I., Eleftheriou, A., and Gaitanakis, P., 1984. 1:50000 Geological Map
908 “Kaparellion”, IGME

909 Caputo, R., Chatzipetros, A., Pavlides, S. & Sboras, S., 2013. The Greek Database of
910 Seismogenic 805 Sources (GreDaSS): state-of-the-art for northern Greece. Annals
911 of Geophysics, 55 (5), 859-894.

912 Chatzipetros, A., Kokkalas, S., Pavlides, S. and Koukouvelas, I., 2005. Palaeoseismic
913 data and their implication for active deformation in Greece. Journal of
914 Geodynamics 40, 170–188.

915 Chen, W.P. and Molnar, P., 1983. Focal depths of intracontinental and intraplate
916 earthquakes and their implications for the thermal and mechanical properties of the
917 lithosphere. Journal of Geophysical Research 88(B5), pp. 4183-4214.

918 Collier, R.E.L, Pantosti, D., D'Addezio, G., De Martini, P.M., Masana, E., and
919 Sakellariou, D., 1998. Paleoseismicity of the 1981 Corinth earthquake fault:

920 Seismic contribution to extensional strain in central Greece and implications for
921 seismic hazard. Journal of Geophysical Research 103(B12), pp. 30001-30019.

922 Cowie, P. A., and Roberts, G. P., 2001. Constraining slip rates and spacings for active
923 normal faults. Journal of Structural Geology 23, pp. 1901-1915.

924 Cowie, P.A. and Shipton, Z.K., 1998. Fault tip displacement gradients and process
925 zone dimensions. Journal of Structural Geology 20(8), pp. 983-997.

926 Darragh, R.B., Bolt, B.A., 1987. A comment on the statistical regression relation
927 between earthquake magnitude and fault rupture length. Bulletin of the
928 Seismological Society of America 77, pp. 1479–1484.

929 Degg, M., 1992. Natural Disasters: Recent trends and future prospects. Geography
930 77(3), pp.198-209.

931 Dounas, A., 1971. 1:50000 Geological Map “Erythrai”, IGME

932 Ellsworth, W.L., Matthews, M.V., Nadeau, R.M., Nishenko, S.P., Reasenberge, P.A.,
933 Simpson, R.W., 1999. A physically-based earthquake recurrence model for
934 estimation of long-term earthquake probabilities. U.S. Geological Survey Open
935 File Report 99-552. 23p.

936 Gaitanakis, I., 1982. 1:50000 Geological Map “Athina-Peiraias”, IGME

937 Gaitanakis, I., Mettos, A., Koutsouvelis, A. and Rontoyiannis, Th., 1984. 1:50000
938 Geological Map “Megara”, IGME

939 Gaitanakis, P., Mettos, A. and Fytikas, M., 1985. 1:50000 Geological Map “Sofikon”,
940 IGME

941 Galanopoulos, A., 1961. A Catalogue of Shocks with Io ≥VII for the Years Prior to
942 1800. National Observatory of Athens, Seismological Institute.

943 Ganas, A. and Athanassiou, E., 2000. A comparative study on the production of
944 satellite orthoimagery for geological remote sensing. Geocarto International 15 (2),
945 pp.51-59.

946 Ganas, A. and Papoulia, I., 2000. High-resolution, Digital Mapping of the Seismic
947 Hazard within the Gulf of Evia Rift, Central Greece using normal fault segments as
948 line sources. Natural Hazards 22, pp. 203–223.

949 Ganas, A., Pavlides, S.B., Sboras, S., Valkaniotis, S., Papaioannou, S., Alexandrisb,
950 G.A., Plessa, A., and Papadopoulos, G.A. 2004. Active fault geometry and
951 kinematics in Parnitha Mountain, Attica, Greece. Journal of Structural Geology 26
952 (2004), pp. 2103–2118

953 Ganas, A., Pavlides, S., and Karastathis, V., 2005. DEM-based morphometry of
954 range-front escarpments in Attica, central Greece, and its relation to fault slip rates.
955 Geomorphology 65 (2005), pp. 301–319.

956 Goes, S.D.B., 1996. Irregular recurrence of large earthquakes: an analysis of historic
957 and paleoseismic catalogs. Journal of Geophysical Research 101, pp. 5739–5749.

958 Goldsworthy, M., Jackson, J., and Haines, J., 2002. The continuity of active fault
959 systems in Greece. Geophysical Journal International 148, pp. 596–618.

960 Grützner, Ch., Barba, S., Papanikolaou, I., Perez-Lopez, R., 2013. Earthquake
961 Geology: science, society and critical facilities. Annals of Geophysics 56 (6),
962 S0683, doi: 10.4401/ag-6503.

963 ~~Grützner, Ch., Schneiderwind, S., Papanikolaou, I., Pallikarakis, A., and~~
964 ~~Deligiannakis, G., 2013. Neotectonic activity of the Milesi Fault, N Attica, Greece.~~
965 ~~In: Grützner, Ch., Rudesdorf, A., Perez – Lopez, R., Reicherter, K. (eds). Seismic~~
966 ~~Hazard, Critical Facilities and Slow Active Faults, Proceedings of the 4th~~

~~International INQUA Meeting onPaleoseismology, Active Tectonics and Archeoseismology.~~

Grützner, C., Schneiderwind, S., Papanikolaou, I., Deligiannakis, G., Pallikarakis, A. & Reicherter, K., 2016. New constraints on extensional tectonics and seismic hazard in northern Attica, Greece - the case of the Milesi Fault. Geophysical Journal International 204, 180–199. doi: 10.1093/gji/ggv443.

Jackson, J.A. and White, N. J., 1989. Normal faulting in the upper continental crust: observations from regions of active extensions. Journal of Structural Geology 11(1/2), pp. 15-36

Jackson, J.A., Gagnepain, J., Houseman, G., King, G.C.P., Papadimitriou, P., Soufleris, C. & Virieux, J. 1982. Seismicity, normal faulting and the geomorphological development of the Gulf of Corinth (Greece): the Corinth earthquakes of February and March 1981. Earth and Planetary Science Letters 57, 377–397.

Katsikatsos, G., 1991. 1:50000 Geological Map “Rafina”, IGME

Katsikatsos, G., 2000. 1:50000 Geological Map “Eretria”, IGME

Katsikatsos, G., 2002. 1:50000 Geological Map “Kifissia”, IGME

Katsikatsos, G., Mettos, A., Vidakis, M. and Dounas, A., 1986. 1:50000 Geological Map “Athina-Elefsis”, IGME

Kokkalas, S., Pavlides, S., Koukouvelas, I., Ganas, A., and Stamatopoulos, L, 2007. Paleoseismicity of the Kaparelli fault (eastern Corinth Gulf): evidence for earthquake recurrence and fault behavior. Italian Journal of Geosciences, 126(2), pp. 387-395.

990 Latsoudas, Ch., 1992. 1:50000 Geological Map “Koropi-Plaka”, IGME

991 Lekkas, E., 2000. The Athens earthquake (7 September 1999): intensity distribution
992 and controlling factors. Engineering Geology 59, pp. 297-311.

993 Machette, M., 2000. Active, capable, and potentially active faults – a paleoseismic
994 perspective. Journal of Geodynamics, 29, pp. 387-392.

995 ~~Main, I., 1996. Statistical Physics, Seismogenesis and seismic hazard. Reviews of~~
996 ~~Geophysics 34, pp. 433-462~~.

997 Makropoulos, K., Burton, P., 1984. Seismic Hazard in Greece. I. Magnitude
998 recurrence. Tectonophysics 117(1985), pp.205-257.

999 Marinos, P., Boukouvalas, G., Tsiambaos, G., Pronotarios, G., and Sabatakakis,
1000 N.,1999b. Damage distribution in the western part of Athens after the 7-9-99
1001 earthquake. Newsletter of E.C.P.F.E., Council of Europe, Issue No 3, 36-39.

1002 Marinos, P., Boukovalas, G., Tsiambaos, G., Protonotarios, G., and Sabatakakis, N.
1003 1999a. Preliminary geological - geotechnical study of the disaster area (of Athens
1004 earthquake of Sept 7th, 1999) in NW Athens Basin. Ministry of Environment,
1005 Planning and Public Works.

1006 Mariolakos, I., Fountoulis, I. and Theocharis, D., 2001. Neotectonic structure and
1007 evolution of the Salamina island. Bulletin of the Geological Society of Greece,
1008 Proceedings of the 9th International Congress, Athens, September 2001, XXIV/1,
1009 pp. 165-173.

1010 Michetti, A.M., Audemard, F.A. and Marco, S. 2005. Future trends in
1011 paleoseismology: Integrated study of the seismic landscape as a vital tool in
1012 seismic hazard analyses. Tectonophysics 408, pp. 3-21.

1013 Michetti, A.M., Esposito, E., Guerrieri, L., Porfido, S., Serva, L., Tatevossian, R.,
1014 Vittori, E., Audemard, F., Azuma, T., Clague, J., Comerci, V., Gurpinar, A.,
1015 McCalpin, J., Mohammadioun, B., Morner, N.A., Ota, Y., Roghozin, E., 2007.
1016 Intensity scale ESI 2007. In: Guerrieri, L., Vittori, E. (Eds.), Memorie Descrittive
1017 Carta Geologica d'Italia. Servizio Geologico d'Italia, vol. 74. Dipartimento Difesa
1018 del Suolo, APAT, Roma, p. 53.

1019 Michetti, A.M., Ferreli, L., Esposito, E., Porfido, S., Blumetti, A.-M., Vittori, E.,
1020 Serva, L., and Roberts, G.P., 2000. Ground effects during the 9 September 1998,
1021 Mw = 5.6, Lauria earthquake and the seismic potential of the "Aseismic" Pollino
1022 region in Southern Italy. Seismological Research Letters 71, pp. 31–46.

1023 Morewood, N. C., and G. P. Roberts (1999). Lateral propagation of the surface trace
1024 of the South Alkyonides fault, central Greece: Its impact on models of fault growth
1025 and displacement-length relationships, Journal of Structural Geology 21, 635–652.

1026 Morewood, N.C., and Roberts, G.P., 2002. Comparison of surface slip and focal
1027 mechanism slip data along normal faults: an example from the eastern Gulf of
1028 Corinth, Greece. Journal of Structural Geology 23 (2001), pp. 473-487.

1029 Musson, R.M.W., Grünthal, G., and Stucchi, M., 2010. The comparison of
1030 macroseismic intensity scales. Journal of Seismology 14, pp. 413–428

1031 Ogata, Y., 1999. Estimating the hazard of rupture using uncertain occurrence times of
1032 paleoearthquakes. Journal of Geophysical Research 104, 17995–18014.

1033 Pace, B., Peruzza, L. and Visini, F., 2010. LASSCI2009.2: layered earthquake rupture
1034 forecast model for central Italy, submitted to the CSEP project. Annals of
1035 Geophysics 3, pp.85-97.

1036 Pantosti, D.R., Collier, G., D'Addezio, G., Masana, E., and Sakellariou, D., 1996.
1037 Direct geological evidence for prior earthquakes on the 1981 Corinth fault (central
1038 Greece). Geophysical Research Letters 23, pp. 3795-3798.

1039 Paolucci, R., 2002. Amplification of earthquake ground motion by steep topographic
1040 irregularities. Earthquake Engineering and Structural Dynamics. 2002 (31),
1041 pp.1831–1853 (DOI: 10.1002/eqe.192).

1042 Papadopoulos, G., Ganas, A., Pavlides, S., 2002. The problem of seismic potential
1043 assessment: Case study of the unexpected earthquake of 7 September 1999 in
1044 Athens, Greece. Earth Planets Space, 54, pp. 9–18.

1045 Papaioannou, Ch.A., 1984. Attenuation of seismic intensities and seismic hazard
1046 assessment in Greece and the surrounding area. Ph.D. Thessaloniki: University of
1047 Thessaloniki 200p.

1048 Papaioannou, Ch.A., and Papazachos, B.C., 2000. Time-Independent and Time-
1049 Dependent Seismic Hazard in Greece Based on Seismogenic Sources. Bulletin of
1050 the Seismological Society of America, 90 (1), pp. 22–33.

1051 Papanikolaou, D., and Papanikolaou, I., 2007. Geological, geomorphological and
1052 tectonic structure of NE Attica and seismic hazard implications for the northern
1053 edge of the Athens plain. Bulletin of the Geological Society of Greece 40, 425-
1054 438.

1055 Papanikolaou, D., and Royden, L.H., 2007. Disruption of the Hellenic arc: Late
1056 Miocene extensional detachment faults and steep Pliocene-Quaternary normal
1057 faults—Or what happened at Corinth? Tectonics 26 (TC5003), pp.1-16.

1058 Papanikolaou, D., Basi, E.K., Kranis, Ch., and Danamos, G., 2004. Paleogeographic
1059 evolution of the Athens plain from late Miocene until today. Bulletin of the G-
1060 eological Society of Greece vol. XXXVI, pp. 816-825.

1061 Papanikolaou, D., Chronis, G., Likousis, V. & Pavlakis, P., 1989a. Submarine
1062 Neotectonic Map of Saronikos Gulf, 1:100,000, E.P.P.O. – N.C.M.R. & Dpt. Of
1063 Dynamic, Tectonic, Applied Geology (University of Athens).

1064 Papanikolaou, D., Chronis, G., Likousis, V. & Pavlakis, P., with the contribution of
1065 Roussakis, G. & Syskakis, D., 1989b. Submarine Neotectonic Map of South
1066 Evoikos Gulf, 1:100,000, E.P.P.O.

1067 Papanikolaou, D., Lekkas, E., Lozios, S., Papoulia, I. & Vassilopoulou, S. 1995.
1068 Neotectonic Map of Eastern Attica. Use and Applications with the Geographical
1069 Information System. 4th Congress of the Geographical Society of Greece,
1070 Proceedings 240-262.

1071 Papanikolaou, D., Lekkas, E., Sideris, C., Fountoulis, I., Danamos, G., Kranis, C.,
1072 Lozios, S., Antoniou, I., Vassilakis, E., Vasilopoulou S., Nomikou, P.,
1073 Papanikolaou, I., Skourtsos, E., and K. Soukis 1999. Geology and tectonics of
1074 Western Attica in relation to the 7-9-99 earthquake. Newsletter of E.C.P.F.E.,
1075 Council of Europe, Issue No 3, pp.30-34.

1076 Papanikolaou, D., Vassilakis, E., and Parcharidis, I., 1998. Satellite images of short
1077 wavelength radiation for structure detection in shallow waters. Case study: Aegina
1078 – Agistri islands, Saronikos Gulf. Bulletin of the Geological Society of Greece,
1079 XXXII (1), pp. 105-111.

1080 Papanikolaou, I.D., 2003. Generation of high resolution seismic hazard maps through
1081 integration of earthquake geology, fault mechanics theory and GIS techniques in

1082 extensional tectonic settings. Unpublished Ph.D thesis, University of London,
1083 437pp.

1084 Papanikolaou, I.D., 2011. Uncertainty in intensity assignment and attenuation
1085 relationships: How seismic hazard maps can benefit from the implementation of
1086 the Environmental Seismic Intensity scale (ESI 2007). Quaternary International
1087 242 (2011), pp. 42-51

1088 Papanikolaou, I.D., and Papanikolaou, D.I., 2007b. Seismic hazard scenarios from the
1089 longest geologically constrained active fault of the Aegean. Quaternary
1090 International 171-172, pp. 31-44.

1091 Papanikolaou, I.D., Papanikolaou, D.I., Lekkas, E.L., 2009. Advances and limitations
1092 of the Environmental Seismic Intensity scale (ESI 2007) regarding near-field and
1093 far-field effects from recent earthquakes in Greece. Implications for the seismic
1094 hazard assessment. In: Reicherter, K., Michetti, A.M., Silva, P.G. (Eds.),
1095 Paleoseismology: Historical and Prehistorical Records of Earthquake Ground
1096 Effects for Seismic Hazard Assessment. Special Publication of the Geological
1097 Society of London, vol. 316, pp. 11-30.

1098 Papanikolaou, I.D., Roberts, G., Deligiannakis G., Sakellariou, A. and Vassilakis E.,
1099 2013. The Sparta Fault, Southern Greece: From segmentation and tectonic
1100 geomorphology to seismic hazard mapping and time dependent probabilities,
1101 Tectonophysics, http://dx.doi.org/10.1016/j.tecto.2012.08.031

1102 Papanikolaou, I.D., van Balen, R., Silva, P.G., and Reicherter, K., 2015.
1103 Geomorphology of active faulting and seismic hazard assessment: New tools and
1104 future challenges. Geomorphology (in press).

1105 Papazachos B.C. and Papazachou C., 1997. The earthquakes of Greece. Thessaloniki:
1106 Ziti Publications.

1107 Papazachos B.C. and Papazachou C., 2003. The earthquakes of Greece. 3rd ed.
1108 Thessaloniki: Ziti Publications.

1109 Papazachos, B.C., Comninakis, P.E., Karakaisis, G.F., Karakostas, B.G.,
1110 Papaioannou, C.A., Papazachos, C.B. and Scordilis, E.M., 2000. A catalogue of
1111 earthquakes in Greece and surrounding area for the period 550BC-1999,
1112 Publication of the Geophysical Laboratory, University of Thessaloniki.

1113 Papazachos, C.B. and Papaioannou, Ch., 1997. The macroseismic field of the Balkan
1114 area, Journal of Seismology, 1, 181-201.

1115 Papazachos, C.B., 1999. An alternative method for a reliable estimation of seismicity
1116 with an application in Greece and surrounding area. Bulletin of the Seismological
1117 Society of America 89, 111–119.

1118 Papoulia, J., Stavrakakis, G., Papanikolaou, D., 2001. Bayesian estimation of strong
1119 earthquakes in the Inner Messiniakos fault zone, southern Greece, based on
1120 seismological and geological data. Journal of Seismology 5, 233–242.

1121 Papoulis, A., 1991. Probability, random variables, and stochastic processes. McGraw-
1122 Hill Series. 576p.

1123 Parginos, D., Mavridis, A., Bornovas, I., Mettos, A., Katsikatsos, G. and Koukis, G.,
1124 2007. 1:50000 Geological Map “Chalkida”, IGME

1125 Parsons, T., 2005. Significance of stress transfer in time-dependent earthquake
1126 probability calculations. Journal of Geophysical Research 110 (B05S02).
1127 http://dx.doi.org/10.1029/2004JB003190

1128 Pavlides, S., and Caputo, R., 2004. Magnitude versus faults' surface parameters:
1129 quantitative relationships from the Aegean Region. Tectonophysics 380, pp. 159-
1130 188.

1131 Pavlides, S.P., Papadopoulos, G., and Ganas, A., 2002. The Fault that Caused the
1132 Athens September 1999 Ms = 5.9 Earthquake: Field Observations. Natural Hazards
1133 27, pp. 61–84.

1134 ~~PreventionWeb, 2003. Greece Disaster Statistics. [Online]. Available at:~~
1135 ~~http://www.preventionweb.net/english/countries/statistics/?cid=68~~

1136 Reicherter, K., Michetti, A.M., Silva Barroso, P.V., 2009. Paleoseismology: historical
1137 and prehistorical records of earthquake ground effects for seismic hazard
1138 assessment. Special Publication of the Geological Society of London 316, pp.1-10.

1139 ~~Reiter, L., 1990. Earthquake Hazard Analysis. Issues and Insights. New York:~~
1140 ~~Columbia University Press 254pp.~~

1141 ~~Roberts, G. P. and Ganas, A., 2000. Fault-slip directions in central-southern Greece~~
1142 ~~measured from striated and corrugated fault planes: comparison with focal~~
1143 ~~mechanism and geodetic data. Journal of Geophysical Research 105(B10), pp.~~
1144 ~~23,443-23,462.~~

1145 Roberts, G. P., 1996. Variation in fault-slip directions along active and segmented
1146 normal fault systems. Journal of Structural Geology 18, pp. 835-845.

1147 Roberts, G.P., Cowie, P., Papanikolaou, I., and Michetti, A.M., 2004. Fault scaling
1148 relationships, deformation rates and seismic hazards: An example from the Lazio-
1149 Abruzzo Apennines, central Italy. Journal of Structural Geology 26, pp.377-398.

1150 Roberts, G.P., Houghton, L., Underwood, C., Papanikolaou, Cowie, P.A., Van
1151 Calsteren, P, Wigley, T., Cooper, F.J., and McArthur, J.M. 2009. Localization of

1152 Quaternary slip rates in an active rift in 10^5 years: An example from central Greece
1153 constrained by ^{234}U-^{230}Th coral dates from uplifted paleoshorelines. Journal of
1154 Geophysical Research 114 (B10406).

1155 Roberts, G., Papanikolaou, I., Vött, A., Pantosti, D., and Hadler, H., (2011). *Active*
1156 *Tectonics and Earthquake Geology of the Perachora Peninsula and the Area of the*
1157 *Isthmus, Corinth Gulf, Greece*. Athens: INQUA -TERPRO Focurs Area on
1158 Paleoseismology and Active Tectonics & IGCP-567 Earthquake Archaeology. p40.

1159 Rondoyanni, T. and Marinos, P. The Athens–Corinth highway and railway crossing a
1160 tectonically active area in Greece. Bulletin of Engineering Geology and the
1161 Environment 67, pp. 259–266.

1162 Sakellariou, D., Lykousis, V., Alexandri, S., Kaberi, H., Rousakis, G., Nomikou, P.,
1163 Georgiou, P., and Ballas, D., 2007. Faulting, seismic-stratigraphic architecture and
1164 Late Quaternary evolution of the Gulf of Alkyonides Basin-East Gulf of
1165 Corinth,Central Greece. Basin Research 19, pp.273–295

1166 Serva, L., 1994. Ground effects in the intensity scales. Terra Nova 6, 414e416.

1167 Serva, L., Esposito, E., Guerrieri, L., Porfido, S., Vittori, E., and Commerci, V., 2007.
1168 Environmental effects from five historical earthquakes in southern Apennines
1169 (Italy) and macroseismic intensity assessment: Contribution to INQUA EEE Scale
1170 project. Quaternary International, 173–174, pp. 30–44.

1171 Sibson, R.H., 1984. Roughness at the base of the seismogenic zone: contributing
1172 factors. Journal of Geophysical Research 89, pp. 5791–5799.

1173 Silva, P.G., Rodriguez Pascua, M.A., et al. 2008. Catalogación de los efectos
1174 geologicos y ambientales de los terremotos en Espana en la escala ESI-2007 y su
1175 aplicación a los estudios paleosismologicos. Geotemas 6, pp. 1063-1066.

1176 Skarlatoudis, A.A., Papazachos, C.B., Margaris, B.N., Theodulidis, N., Papaioannou,
1177 Ch., Kalogeras, I., Scordilis, E.M. and Karakostas V., 2003. Empirical peak
1178 ground-motion predictive relations for shallow earthquakes in Greece. Bulletin of
1179 the Seismological Society of America 93(6), 2591-2603.

1180 Stein, R.S., 2003. Earthquake conversations. Scientific American 60–67.

1181 Stein, S., Geller, R.J., Liu, M., 2012. Why earthquake hazard maps often fail and what
1182 to do about it. Tectonophysics 562-563, 1-25.

1183 Stucchi, M., Rovida, A., Gomez Capera, A.A., Alexandre, P., Camelbeeck, T.,
1184 Demircioglu, M.B., Gasperini, P., Kouskouna, V., Musson, R.M.W., Radulian, M.,
1185 Sesetyan, K., Vilanova, S., Baumont, D., Bungum, H., Fäh, D., Lenhardt, W.,
1186 Makropoulos, K., Martinez Solares, J.M., Scotti, O., Živcic, M., Albini, P., Batllo,
1187 J., Papaioannou, C., Tatevossian, R., Locati, M., Meletti, C., Viganò, D., and
1188 Giardini, D., 2012. The SHARE European Earthquake Catalogue (SHEEC) 1000-
1189 1899. Journal of Seismology 17, 523-544.

1190 Tataris, A., Kounis, G. and Maragkoudakis, N., 1966. 1:50000 Geological Map
1191 “Thivai”, IGME

1192 Tatevosian, R.E., 2007. The Verny, 1887, earthquake in Central Asia: Application of
1193 the INQUA scale, based on coseismic environmental effects. Quaternary
1194 International, 173–174, pp.23–29.

1195 Theocharis, D., and Fountoulis, I., 2002. Morphometric indices and active tectonic
1196 structures. The case of Salamina. Proceedings of the 6th panhellenic geographical
1197 conference of the Hellenic Geographical Society, I, pp. 97-106.

1198 Theodulidis, N. P. and Papazachos, B.C., 1992. Dependence of strong ground motion
1199 on magnitude-distance, site geology and macroseismic intensity for shallow

earthquakes in Greece: I, Peak horizontal acceleration, velocity and displacement. Soil Dynamics and Earthquake Engineering 11(1992), pp.387-402.

Theodulidis, N. P., 1991. Contribution to strong ground motion study in Greece. Ph.D. Thessaloniki. University of Thessaloniki.

Tsodoulos I.M., Koukouvelas, I.K., and Pavlides, S., 2008. Tectonic geomorphology of the easternmost extension of the Gulf of Corinth (Beotia, Central Greece). Tectonophysics 453 (2008), pp. 211–232.

Udias, A., 1999. Principles of Seismology. Cambridge University Press. 475p.

Wald, D.J., Quitoriano, V., Heaton, T.H., Kanamori, H., 1999. Relationships between peak ground acceleration, peak ground velocity, and modified Mercalli intensity in California. Earthquake Spectra 15, pp. 557–564.

Wells, D.L. and Coppersmith, K., 1994. New Empirical Relationships among Magnitude, Rupture Length, Rupture Width, Rupture Area, and Surface Displacement. Bulletin of the Seismological Society of America 84(4), pp. 974-1002.

Wesnousky, S.G. (1987), Geological Data and Seismic Hazard Analysis: Past and Future, Proceedings of Conference XXXIX, Directions in Paleoseismology, U.S.G.S. Open-File Report 87-673, pp. 418-427.

Working Group on California Earthquake Probabilites (WGCEP), 1990. Probabilities of large earthquakes in the San Fransisco Bay region, California. U.S. Geol. Surv. Circ., 1053, 51pp.

Working Group on California Earthquake Probabilities (WGCEP), 1999. Preliminary report: Earthquake Probabilities in the San Francisco Bay Region: 2000-2030 - A Summary of Findings. USGS Open-File Report 99-517.

Working Group on California Earthquake Probabilities (WGCEP), 2002. Earthquake probabilities in the San Francisco bay region: 2002-2031. USGS Open-File Report 03-214.

Working Group on California Earthquake Probabilities (WGCEP), 2007. Uniform California Earthquake Rupture Forecast 2 Final Report.

Yeats, R.S., and Prentice, C.S., 1996. Introduction to special section: Paleoseismology. Journal of Geophysical Research 101, pp. 5847-5853.

~~Youngs, R. R. and Coppersmith, K. J., 1985. Implications of fault slip rates and earthquake recurrence models to probabilistic seismic hazard estimates. Bulletin of the Seismological Society of America 75(4), pp. 939-964.~~